PNL-8046
UC-704

PNL--8046

DE93 007771

PELLET RELOCATION TESTING RESULTS FOR FOUR-FOOT-LONG TRITIUM TARGET RODS

M. A. McKinnon
N. E. Harding

May 1992

Prepared for
the U.S. Department of Energy
under Contract DE-AC06-76RLO 1830

Pacific Northwest Laboratory
Richland, Washington 99352

SUMMARY

Four-foot-long sections of a new production light-water reactor (NP-LWR) generic tritium target rod were tested to determine if the length of the pellet pencils affects the amount of pellet material relocated during a burst and to characterize the burst. This testing was conducted as a follow-on study of cladding strength and pellet relocation behavior of short target rod specimens [11 cm (4.4 in.)]. The results of these tests could be used to support safety analyses of the effects of rod bursting and pellet relocation on the performance of a NP-LWR reactor core during a postulated loss-of-coolant accident (LOCA). All burst tests of the target rods were performed in air because air is more reactive than the air-steam or water environment that accompanies a LOCA.

Four tests were conducted at four different backfill pressures varying from 1000 psia to 3000 psia. During these tests, target rod specimens with four pencils were charged with helium gas and then inductively heated using a 5.6°C/sec (10°F/sec) ramp rate until they burst. The pencils were comprised of pellets, getters with bent tabs, and liners identical in transverse cross section and length to a generic target rod design. Previous testing used three short pencils whose combined length was 4.6 in. compared to the four prototypic foot-long pencils used in this testing. The same induction coil used in previous tests with shorter target rod specimens was used for heating the cladding. Consequently, only a small portion of each specimen was heated. This heated zone was approximately the same length and had the same axial temperature profile in the burst zone as was used for the shorter specimens. The test results indicate that the strength of 20% cold-worked barrier coated stainless steel cladding (pressure-temperature threshold for cladding breach) is not significantly affected by the volume of gas in the specimen. The test results also show that pellet damage is confined to the pencil at the burst location for the pressures and axial temperature profile used in testing.

Post-test radiographs indicate that the short heated length of the rods may have limited pellet relocation. The structural strength of the nickel-plated Zircaloy getter may be important in limiting pellet relocation. In

general, pellet material was ejected from the pencil at the burst location, and the pencil above the burst location moved down to fill the void. The plenum spring can follow or drive the pencil downward.

The test specimens and test conditions are described in the body of the report. Results of the testing are summarized in the conclusion and recommendation section of the report.

ACKNOWLEDGMENTS

The authors would like to thank the U.S. Department of Energy, Office of New Production Reactors, for sponsoring this work. Thanks are also extended to E. R. Gilbert of Pacific Northwest Laboratory's Tritium Target Development Project. Appreciation is extended to N. S. Cannon for help with the data acquisition system, J. O. Vining for specimen component fabrication, L. J. Parchen for specimen assembly and characterization, R. F. Klein and F. D. Hobbs for welding support, and R. C. Pedersen for editorial support.

CONTENTS

FIGURES

TABLES

1.0 INTRODUCTION

The Code of Federal Regulations, 10CFR50 Appendix A (Criteria 27 and 35), and national standards ANS/ANSI-51-1 require that coolable geometry and reactivity control in a reactor core are not compromised during a large break loss-of-coolant accident (LBLOCA). A primary safety concern is to prevent events that are design-basis accidents in a commercial light-water reactor (LWR) from becoming severe accidents in the new production reactor (NPR) design.

During a postulated loss-of-coolant accident (LOCA) in a nuclear reactor, the temperatures of the fuel and tritium target rods in the reactor core will significantly exceed their normal operating temperatures. The magnitude of the elevated temperature of the target rods depends on the reactor core design. Analyses results associated with current reactor core designs do not result in temperatures sufficient to cause the cladding of target rods to breach. Moreover, previous experiments conducted on target rod materials at postulated transient temperatures and pressures established the cladding breach temperature and pressure thresholds. These thresholds are above predicted temperatures and pressures for a postulated LOCA.

However, if future target rod designs resulted in the possibility of a cladding breach (burst), it would be important to characterize the pellet relocation associated with a burst. Because the lithium aluminate pellets in the rods act as a neutron poison, their relocation during a burst can affect the reactivity of the core. If significant amounts of lithium aluminate pellet material were relocated when the rod cladding burst, then the relocated material could affect further fission reactions in the core. Voids in the tritium target rods left by the relocated lithium aluminate would not absorb neutrons from the fission chain reaction; these voids could increase core reactivity.

To characterize the pellet relocation behavior of target rods during a burst, Pacific Northwest Laboratory[a] has conducted out-of-reactor burst tests on target rod specimens at postulated transient temperatures and pressures. This study extends the results of previous tests by using longer specimens with pencils that are of prototypic length. The primary objective of this study was to determine whether pellet relocation is confined to the pencil at the burst location when the pencils are of prototypic length. The results of these out-of-reactor tests could support plant safety analyses to determine the effects of replacing certain fuel rods with tritium target rods in a reactor core and to predict the behaviors of reactor core cooling and recriticality if tritium target rods burst during postulated LOCA conditions.

Previous testing addressed the effect of the barrier coating on cladding strength when the target rod was subjected to extreme transient temperatures and pressures (McKinnon 1992). The previous tests used short target rod specimens [11-cm (4.4-inch) heated cladding length] which were charged with helium gas and then inductively heated to the point of bursting. A temperature ramp rate of 5.6°C/sec (10°F/sec) was achieved during the heating process. The short specimens for pellet relocation studies contained three pencils (composed of getters, pellets, and inner liners). All of the burst tests were performed in air.

This report compares the strength and pellet relocation results of current testing effort with the results from the previous testing. The conclusions and recommendation from the testing are presented in Section 2.0. Section 3.0 describes specimen designs, test temperatures and pressures, the test apparatus, and the test plan. Section 4.0 presents the test results with supporting discussions. Lastly, Appendix A contains data from the 4-ft tritium target burst tests. These data include burst temperatures and pressures, volume, weight, and dimensional changes of the target rod specimens. Appendix B presents an error analysis.

(a) Pacific Northwest Laboratory is operated by Battelle Memorial Institute for the U.S. Department of Energy under Contract DE-AC06-76RLO 1830.

2.0 CONCLUSIONS AND RECOMMENDATION

Burst testing successfully demonstrated that pellet damage was confined to the pencil at the burst. The results from testing 4-ft specimens were not significantly different than those from testing the shorter specimens. However, the short heated zone used during the test did not allow us to determine the total extent of the damage that could occur for a full length target rod with a prototypic axial temperature distribution. It was apparent from the test that the strength of the nickel-plated getter may influence the pellet release associated with a burst.

The following subsections present specific conclusions and a recommendation developed from the test results.

2.1 CONCLUSIONS

The results of the ex-reactors burst tests lead to the following conclusions.

- The burst strength, diameter change, and breach damage to the cladding of the 4-ft specimens were the same as observed for burst testing with shorter specimens.
- Pellet and pencil damage is confined to the pencil at the burst location. Burst damage does not propagate to adjoining pencils for the pressures tested.
- The length of the heated zone may affect pellet relocation. Using the same heated length, approximately the same length of pellet column within the heated zone was expelled from the 4-ft specimens as had been expelled from shorter specimens. There is no indication of pencil damage outside of the heated zone.

2.2 RECOMMENDATION

The results of the ex-reactor burst tests lead to the following recommendation:

- Tests should be conducted with specimens having longer heated zones. To determine pellet relocation from a target rod, the heated zones need to have prototypical axial temperature profiles (length and temperature).

3.0 TESTING

This section describes specimen designs, test temperatures and pressures, the test apparatus, and the test plan.

3.1 TEST SPECIMENS

Several test specimen designs have been used in the ex-reactor safety testing portion of the Tritium Target Development Project (TTDP). Each has incorporated the design features of the generic target rod (Shiraga and Weber 1991). This section describes the generic target rod design and the other designs as they have evolved over the testing span. The 4-ft target rod specimen used in the performance testing is also described.

3.1.1 Generic Target Rod Design

The generic target rod is shown in Figure 1. The nominal dimensions of the cladding, nickel plated Zircaloy (NPZ) getter, $LiAlO_2$ pellets, and inner liner are summarized in Table 1. The generic target rod contains 12 pencils of 30.5 cm length, end caps, and a compression spring as shown in the Figure 1.

The earliest tests were performed with the specimens shown in Figure 2. The specimens had about 12 cm (4.6 inches) of barrier coated stainless steel cladding, contained a filler rod to limit gas volume, and were used to determine the effect on cladding strength of the barrier cladding and its associate heat treatment. This specimen was heated using an induction heater. A heating coil used with the induction heater was fabricated to produce a flat temperature profile within ±27.8°C (±50°F) of the mean temperature over the center 7.6 cm (3 inches) of the specimens cladding. This left very little of the short specimen that was not heated.

The next specimen design included pellets, a NPZ getter, and an inner liner. It is shown in Figure 3 and was used for the initial pellet relocation burst testing. It did not include pencil tabs or gas plenums.

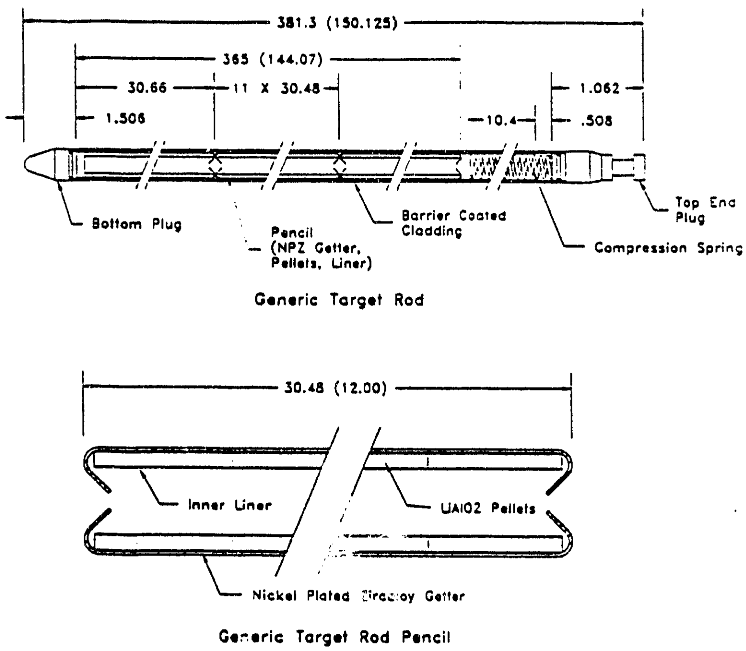

FIGURE 1. Generic Target Rod Design

TABLE 1. Target Rod Nominal Dimensions

Feature	Dimension, mm (inch)	Drawing Number
Barrier Coated 316 SS Cladding OD[a]	9.423 (0.371 ± 0.001)	4D02256, Rev. 3
Barrier Coated 316 SS Cladding ID	8.280 (0.326 ± 0.001)	4D02256, Rev. 3
Nominal Cladding Barrier Thickness OD	0.0127 (0.0005)	4D02256, Rev. 3
Nominal Cladding Barrier Thickness ID	0.0508 (0.002)	4D02256, Rev. 3
Nickel Plated Zircaloy-4 Getter OD	8.128 (0.320 ± 0.0015)	4D02259, Rev. 2
Nickel Plated Zircaloy-4 Getter ID	7.798 (0.307 ± 0.002)	4D02259, Rev. 2
Nickel Plating Thickness	0.0051 (0.0002 >0.0012)	4D02259, Rev. 2
Target Pellet OD	7.645 (0.301 ± 0.0015)	6945C65, Rev. 1
Target Pellet ID	5.613 (0.221 ± 0.003)	6945C65, Rev. 1
Inner Liner Thickness	0.1016 (0.004)	4D02259, Rev. 2
Specimen Gas Volume	8.6 cc (0.52 cubic inches)	

(a) ID = inner diameter.
OD = outer diameter.
Note: Shroud dimension was adjusted to maintain a 0.889-mm (0.035-inch) gap between the shroud and the target cladding.

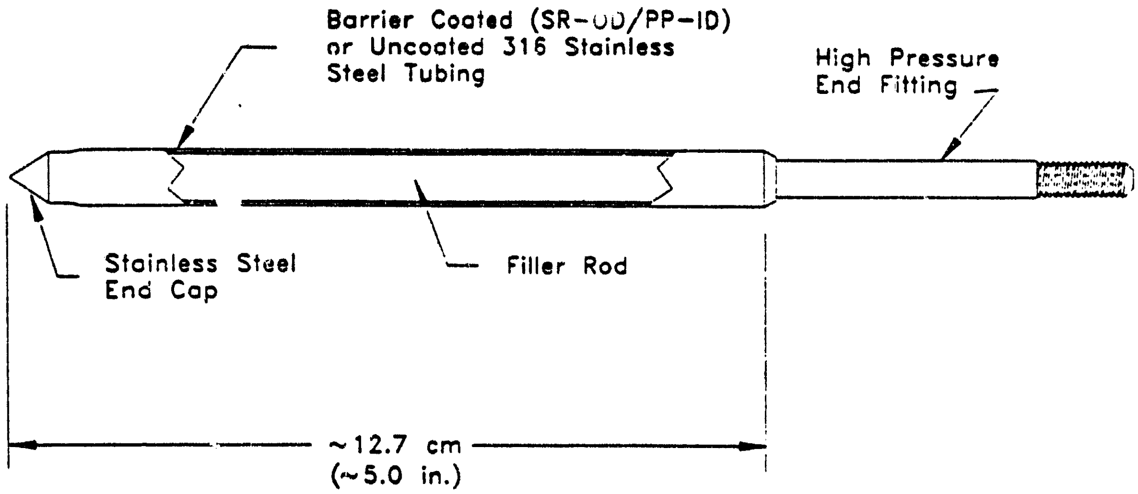

FIGURE 2. Transient Burst Specimen with Internal Filler Rod

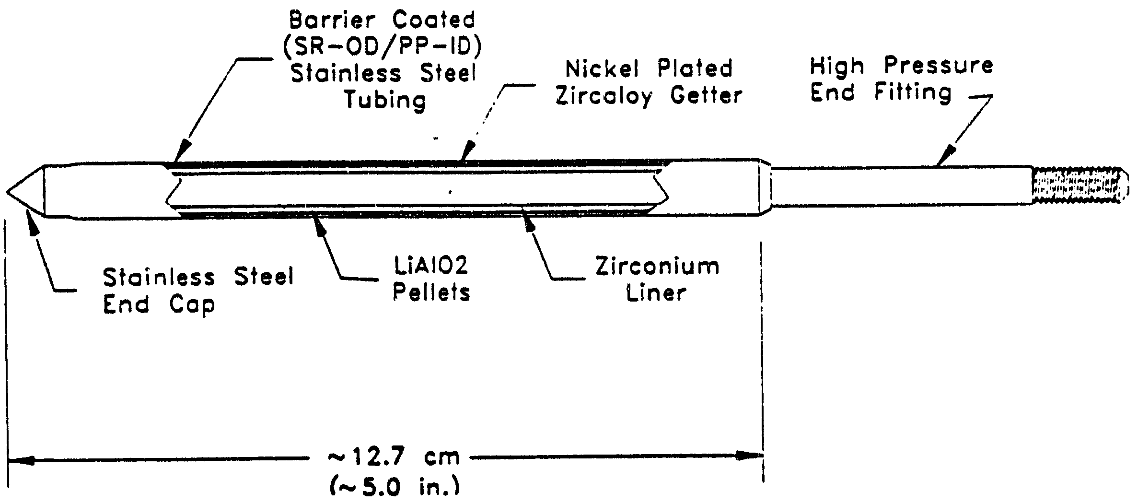

FIGURE 3. Transient Burst Specimen with Internal Target Rod Components

The specimen illustrated in Figure 4 was tested to include more of generic target rod design features. This specimen had transverse cross sections prototypic of the generic rod design (Table 1) and included three pencils. To test the specimen with the same induction heater and heater coil, the pencils were shortened to 2 and 7 cm (0.82 and 2.72 inches) respectively. The pencils included the bent tabs so that gas flows, shock waves, and effects of shock waves caused by the change in flow areas at the pencil interfaces

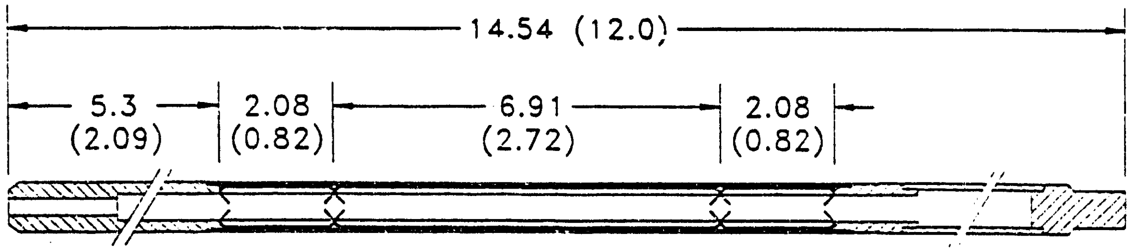

FIGURE 4. One-Foot Target Rod Pellet Relocation Specimen

would be more prototypic of a long target rod. The specimen included a short plenum region to provide flow through all of the pencils. The gas plenums were outside the heated zone during testing. Tests with this specimen indicated that pellet damage was confined to the pencil at the burst location. However, the shortness of the pellet pencils and the lack of a plenum spring prohibited extrapolating pellet damage to the longer generic rods. None of the specimens had included the plenum spring. There was some concern that the plenum spring assembly could act as a gas piston which would drive additional pencil (pellet) material to and out of the breach location.

The next logical extension of the testing was to examine a longer specimen that contained the plenum spring assembly. The design shown in Figure 5 was tested because some longer target rods used in criticality testing performed at the Advanced Test Reactor (ATR) reactor at Idaho National Engineering Laboratory (INEL) were available. This rod design allowed maximum use of components in the ATR target rods. These components included four 30.5-cm (12-inch) pencils per ATR rod and the spring plenum assembly. The pencils include pellets and unplated Zircaloy getters. To make the specimen behave prototypically, inner liners were added to the pencils, one of the unplated getters was replaced with a NPZ getter, and the uncoated stainless steel cladding used in the ATR critical rods was replaced with barrier coated cladding. The NPZ getter was placed in the heated zone.

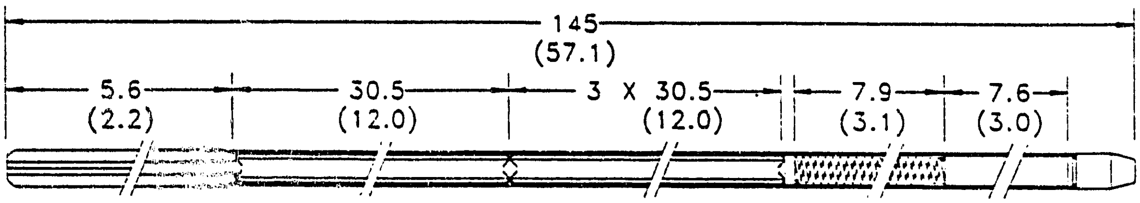

FIGURE 5. Four-Foot Target Rod Pellet Relocation Specimen

In order to determine the effects of the plenum spring assembly and specimen length, the length of the heated zone was not changed. The same heater and heating coil from the prior tests was reused. The heater coil was designed to produce a relatively flat temperature profile within ±27.8°C (±50°F) of the mean temperature over the center 7.6 cm (3 inches) of the specimens. This configuration heated most portions of the short specimens. However, this heated length left most portions of the 4-foot specimen unheated. Using this heated length would simulate actual burst characteristics and allow us to determine if pellet damage was propagated beyond the pencil at the burst location. The heated length was not expected to indicate temperature effects.

The specimen used in this study retained all of the features of the generic rod design except for overall length. It contained four 30.5-cm (12-inch) pellet pencils instead of twelve contained in the generic rod design. Only one of the Zircaloy getters in the specimen was nickel plated. This pencil was positioned in the specimen to be in the heated zone and to provide opportunity for an eutectic formation between the nickel plating and the Zircaloy of the getter. In previous testing, nickel/Zircaloy eutectic appeared to interact with the cladding. The three unplated getters were positioned out of the heated zone. The plenum spring region for the specimen was 7.9 cm long compared to about 11 cm for the generic design.

Bent tabs were included because of their potential impact on the gas dynamics inside the specimen during depressurization following a burst. The tabs form flow restrictions at the ends of each pencil-pellet stack. When the specimen bursts, the flow restrictions can act as a throat or nozzle and may become locations for the attachment of shock waves. For a shock wave to form, the pressure ratio (pressure downstream/pressure upstream) across the shock wave must be less than 0.49 (Owczarek 1964).

When the target cladding breaches, gas will flow out through the burst location. As the downstream pressure decreases, the velocity in the throat (any flow restriction) will increase until sonic velocity is achieved. At sonic velocity, a shock wave will form at the restriction, and the flow rate down the center of the pencil will become independent of further decreases in downstream pressure. The pressure drop across the shock wave can approximate the internal pressure of the target rod just before bursting. In addition, there are several flow paths to the break location (between the cladding and NPZ getter, between the NPZ getter and pellets, and down the center of the pellets). Each of these flow paths could have different locations for shock wave attachments. The location of the shock wave could affect the pressure drop across the various components comprising the target rod. The potential magnitude of the pressure drop could affect the physical integrity of each of the components. For this reason, pencils, pencil tabs, pellets, and liners were considered important design features of the specimens.

3.2 LOCA TEMPERATURE AND PRESSURE RELATIONSHIPS

The LOCA temperatures and pressures used for testing were derived from NPR Tritium Target LOCA Analysis (Omberg 1991). Typical predicted temperature and pressure transients and axial temperature profiles for a target rod shrouded by a guide tube are shown in Figures 6 through 8. Typical temperatures of the fuel, shroud, and target cladding as a function of time for a target shrouded by a guide tube are shown in Figure 6. The maximum cladding temperature for the target is about 790°C (1460°F) about 140 seconds into the transient. The target begins to cool after 140 seconds. The corresponding

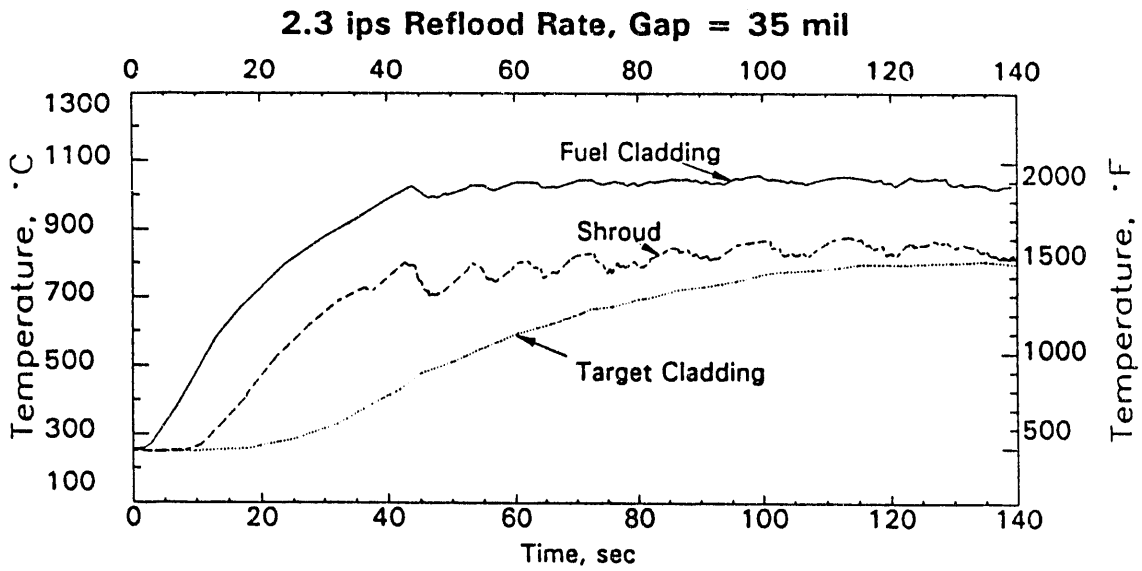

FIGURE 6. LOCA Temperature Transient

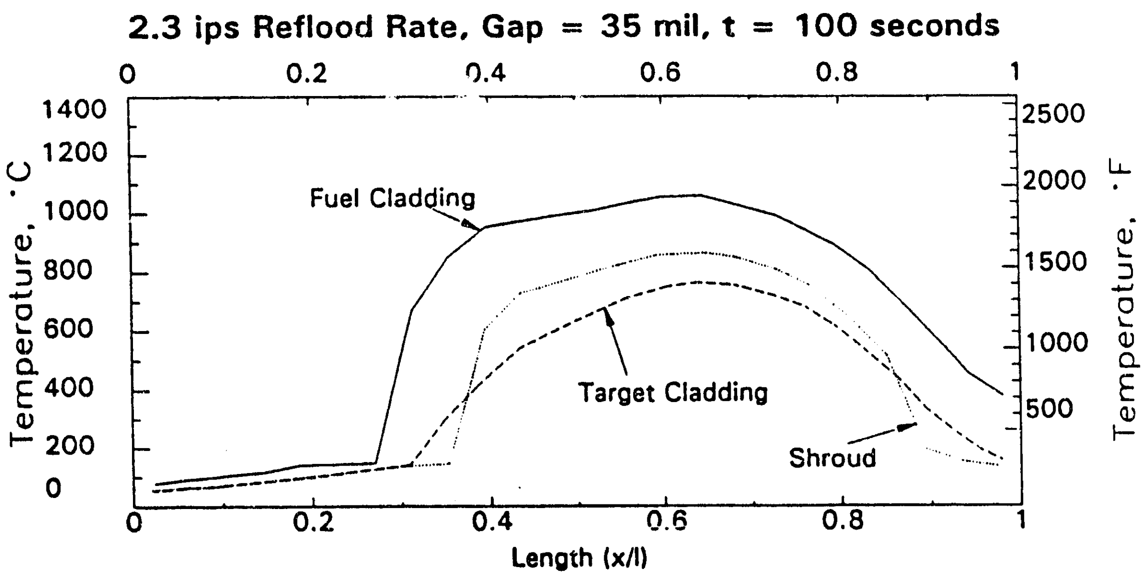

FIGURE 7. Predicted Axial Temperature Profile - Full Length Rod During LOCA

maximum guide tube and fuel temperatures are around 820°C (1510°F) and 1040°C (1900°F), respectively. Other analyses indicated that the maximum target temperature expected for an unshrouded target would be around 1015°C (1860°F). Figure 6 shows where the temperature difference between the target and the

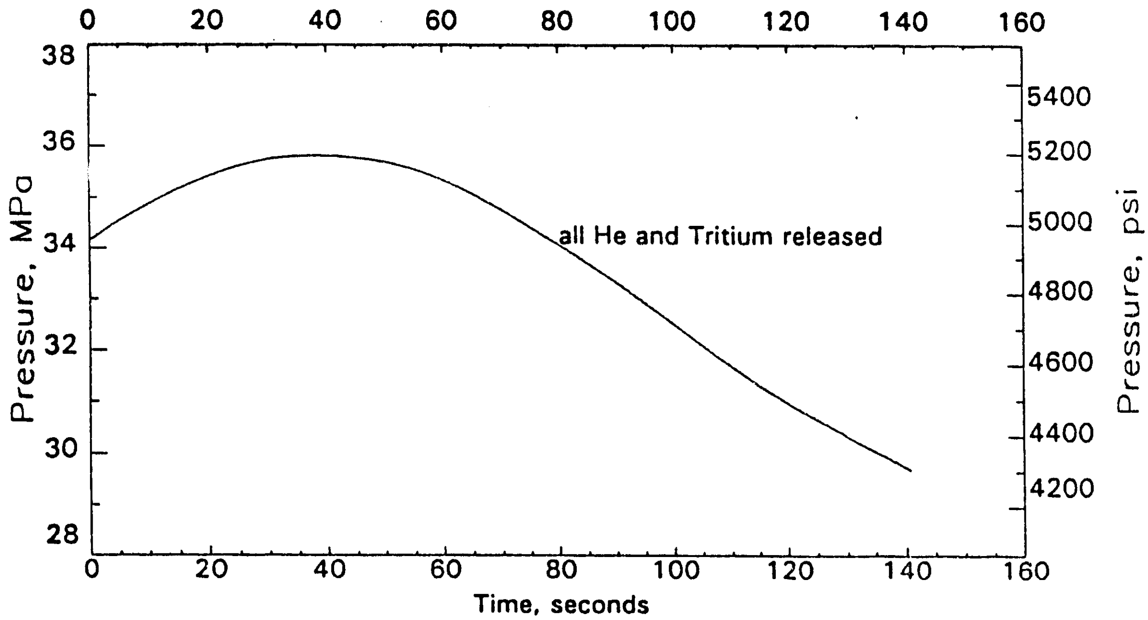

FIGURE 8. Target Rod Pressure Transient in LOCA

shroud (guide tube) varies continuously throughout the transient. The difference can be more than 390°C (700°F) near the beginning of the transient and less than 25°C (50°F) just before cooling.

Figure 7 shows representative axial temperature profiles for the fuel, shroud (guide tube), and target cladding. The target's axial temperature profile was used to calculate the gas pressure in the target as a function of time. As the figure indicates, the cladding and gas in the bottom portion of the target rod are cooled by the reflood. This cooling will reduce the internal gas pressure in the target rod. The resulting pressure profile is shown in Figure 8. For the pressures shown in Figure 8, it was assumed that gas loading at end-of-life conditions was based on an unclassified production rate of 85 million curies of tritium per year. Additionally, it was assumed that all the tritium was released from both the lithium aluminate and the getter, and that all helium was released from the lithium aluminate. The pressures shown represent an upper bound and were used to develop the test matrix.

Gettering of the tritium and gas retention of tritium and helium in the pellets will significantly reduce target rod pressures. Since tritium is heavy hydrogen, gettering of tritium can be inferred from data on gettering of hydrogen. The NPZ getter will absorb large amounts of hydrogen as a result of hydride formation. The equilibrium concentration of hydrogen in the Zircaloy depends on temperature and hydrogen partial pressure. For a given temperature and quantity of hydrogen and zirconium there is an equilibrium partial pressure for hydrogen. The equilibrium partial pressure increases with both temperature and concentration of hydrogen in the zirconium. As the temperature changes, hydrogen in the zirconium will either be absorbed or desorbed. A representative compilation of the data on equilibrium partial pressures of hydrogen in contact with zirconium as a function of temperature is shown graphically in Figure 9.[a] For the target rod design test, the tritium/Zr atom ratio at end-of-life would be less than 0.3. Because only a portion of the rod is hot (>1300°F) during a LOCA (see Figure 7), the tritium driven off at the hot getter locations would be absorbed in the getters at cooler rod locations. If tritium acts similar to hydrogen, then the tritium partial pressure will be low (a few mm Hg). The tritium gettering would reduce the pressures shown in Figure 8 by 30% to 50% resulting in maximum target rod pressures below 20.7 mPa (3000 psi).

3.3 PRETEST AND POST-TEST SPECIMEN CHARACTERIZATION

Both pretest and post-test characterizations of the test specimens were performed so that changes in specimen weight, diameters, and length could be determined after testing. Pretest measurements included internal volume, diameter, length, and weight. In addition, radiographs were taken of specimens containing $LiAlO_2$ pellets for use in post-test analysis of pellet relocations. Follower cards were used to record material sources, cleaning procedures, fabrication procedures, specimen volumes, pre- and post-test measurements, test conditions, and burst temperatures and pressures. Copies of blank follower cards are shown in Appendix A.

(a) J. L. Brimhall, "Test Requirements for Obtaining Data on Tritium/Hydrogen Release from Nickel-Plated Zircaloy (NPZ) and Zirconium," dated June 22, 1990. [Has a list of references on zirconium gettering of hydrogen.]

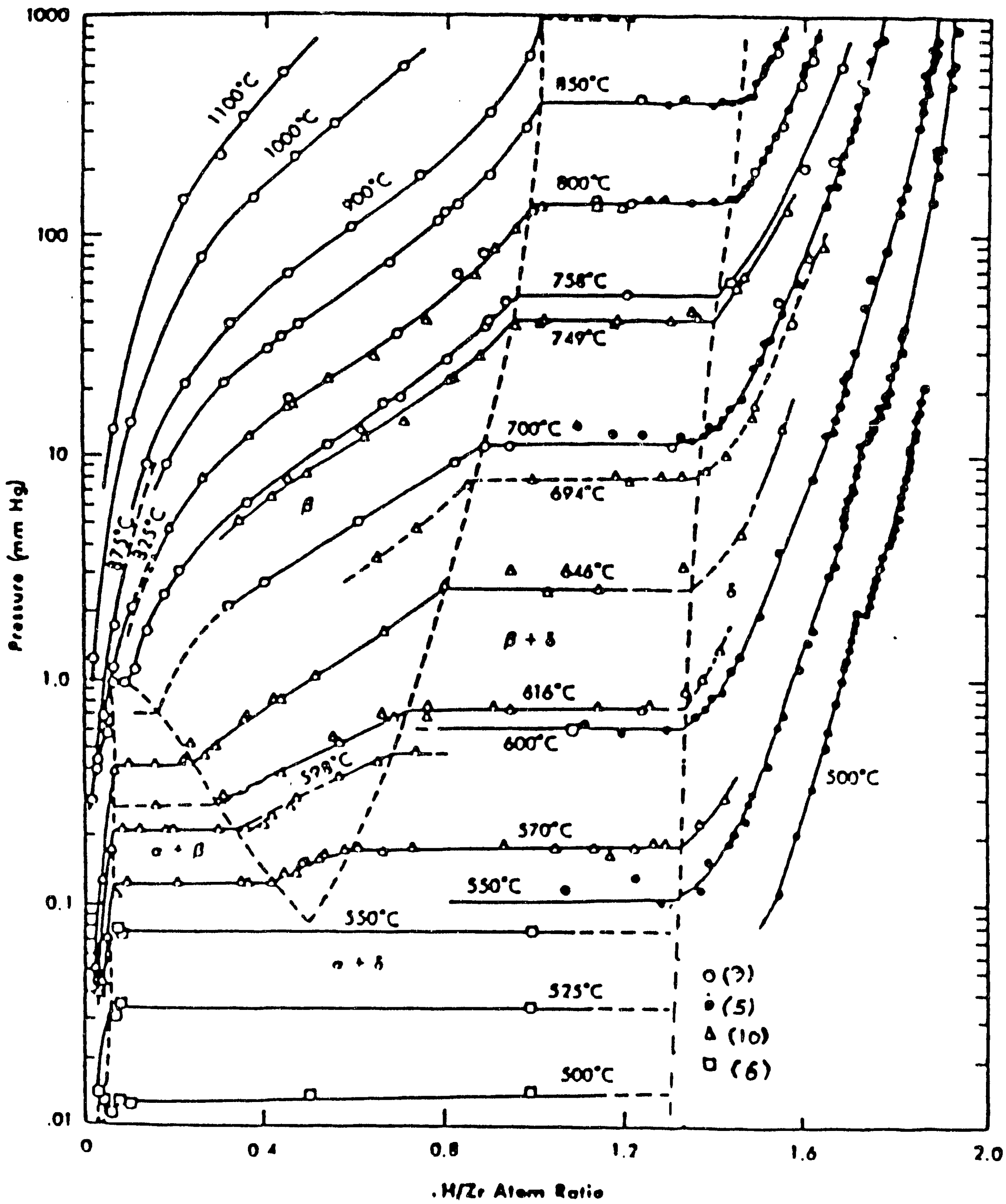

FIGURE 9. Zirconium-Hydrogen Phase Diagram (Carnes and Kherani 1987)

After testing, each specimen's diameter, length, and weight were measured. Radiographs were taken and metallography was performed for specimens containing $LiAlO_2$ pellets. These measurements provided the information that was needed to assess the performance of the specimen.

3.4 TEST APPARATUS DESCRIPTION

The test apparatus consisted of a test stand to hold the specimen, a helium pressurizing system, a LEPEL induction heater, and a computer-controlled data acquisition and control system. The test stand is shown in Figure 10. The test stand had a raised platform that contained a threaded fitting to support the specimen and connect it to the pressurizing system. The test stand also contained metal rods for holding and positioning the induction heater coil, diametrical strain measurement fingers (not used during this program), and a support for a plastic blast-deflection shield. Although the plastic shield is not shown in Figure 10, the figure does show the LEPEL induction heater with its water cooled leads connected to the heating coil.

The helium pressurizing system contained a high pressure cylinder of helium, a Heise pressure gauge that has a National Institute of Standards and Technology (NIST) traceable calibration, and an assortment of valves. The Heise pressure gauge was used as a pressure reference for backfilling the specimen and for calibrating the pressure monitoring system.

The data acquisition and control system used a PDP 11/34 Computer. The computer senses, controls, and records the temperature of the specimen throughout the test. The computer also records the specimen pressure. Temperature is computer controlled through monitoring a thermocouple (TC) attached to the specimen and then by adjusting the power output of the LEPEL induction heater to obtain a fixed temperature ramp rate of 5.6°C/second (10°F/second). This temperature ramp rate is the average rate during a postulated LOCA (Heacock 1991).

The heater coil used for testing the 4-ft rods had been used during previous testing (McKinnon 1992). The coil was made by winding 1/8-in. copper tubing around a mandrel. The coil's axial spacing was adjusted to produce the

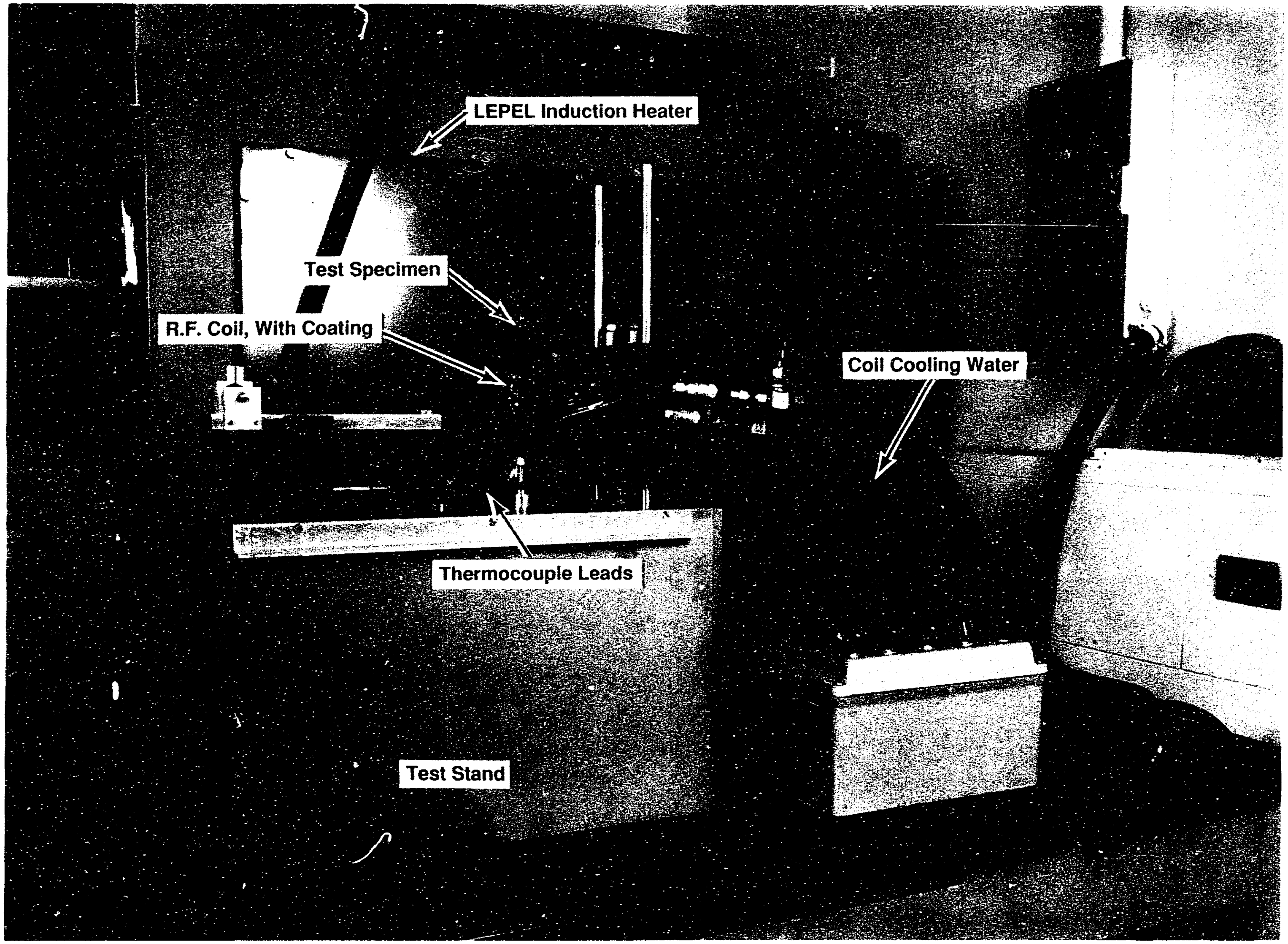

FIGURE 10. Transient Burst Testing Stand

proper axial temperature profile and then was coated with Glyptal[(a)] to hold it together during testing. The inside of the coil was lined with mica sheeting to protect it when the specimens burst. Testing the heater coil's performance consisted of attaching five TCs at 1.9-cm (0.75-in.) intervals on the center portion of the length to be heated. Then the temperature of the specimen was ramped and the five axial temperatures were recorded. The axial spacing between induction heater coils was adjusted until the desired flatness of the temperature profile was achieved. The heater coil used in testing produced temperatures within a 27.3°C (50°F) span over the center 7.6 cm (3 in.) of the specimen. This span falls within the ASTM standard (ASTM E 151) for hot tensile testing.

3.5 TEST PLAN

The test plan required the testing of four 4-ft target rods (Figure 5) using the basic induction heater used for ex-reactor safety tests during 1990 (McKinnon 1992). Testing included pre- and post-test specimen weight and diameter measurements, photographs, and radiographs. Specimen cladding transient temperatures and internal pressure were controlled and monitored during testing. The specimen was pre-charged with helium gas prior to heating. The test plans designated burst pressures of approximately 8, 12, 16.5, 21 MPa (1150, 1750, 2400, 3000 psi). The heated zone was limited to about 15 cm (6 inches) of the specimen cladding and the remainder of the cladding was to remain unheated. The heated zone was heated up to 300°C (572°F), held for 5 minutes, and then ramped at 5.6°C/sec (10°F/sec) until the cladding bursts. The center 7 cm (3 inches) of the heated cladding was kept within the guidance for hot tensile testing provided by ASTM E 151, which specified that the uniformity of temperature shall be within +1.0 and -2.0 percent of the nominal test temperature above 540°C (1000°F). Tests were run in air with helium gas in the target specimen.

The amount of pellet material lost was determined by comparing pretest and post-test weights of the specimens. The source (pretest location) of lost

(a) Insulating paint manufactured by General Electric.

pellet material was determined through examination of post-test radiographs of the specimens. This report documents the test results.

Follower cards were used in the fabrication and testing of the specimens. The follower cards provide traceability between the specimen and a specific design, materials, and all procedures used in its fabrication and testing. The follower card contains pre- and post-test measurements of gas volume, diameter, length, and weight and provides traceability to measurement instruments and procedures. Initial specimen temperature and pressure, ramp rate, and burst temperature and pressure were recorded on the follower card along with name and location of the data file containing the temperature/pressure-time data associated with the test. Testing was conducted according to approved test procedures.

4.0 TEST RESULTS

The transient burst testing of four 4-ft target rods (Figure 5) is an extension of earlier burst testing (McKinnon 1992) using shorter specimens (Figures 2 through 4). The testing was done to determine how longer pencil lengths and the plenum spring assembly affect the relocation of pellet materials from the target rods. This section presents the test results obtained from the 4-ft target rods and compares them with burst data and results collected during previous testing.

4.1 CLADDING BURST STRENGTH

The cladding burst strength for the four specimens tested is compared with the data from previous tests in Figure 11. The four data points generated for the current burst tests are shown as open circles. The data points from the 1990 pellet relocation specimen (Figure 4) are shown as open diamonds connected by dashed lines. This specimen included three short pencils and a small plenum. It did not contain the plenum spring assembly. The data from the specimens show a step decrease in strength at about 1000°C. This step decrease in strength is more evident in the 1990 data than in the current study because of the number of data points and the larger decrease in strength. The step decrease was attributed to the formation of a eutectic between the nickel plating and the Zircaloy of the getter. Evidence of the eutectic, as determined by metallagraphy, is contained in the report of the previous work (McKinnon 1992). The eutectic weakens the stainless steel cladding through liquid-metal embrittlement.

Parts of other important data sets are also shown on Figure 11. They include results of an extensive study by Hunter et al. (1975) used to qualify cladding used in the Fast Flux Test Reactor (FFTF). This data set is represented by a dotted line in Figure 11. The other data shown on Figure 11 were generated in studies supporting the TTDP. The data on 20% cold-worked (CW) (coated or uncoated) cladding was obtained through testing of burst specimens with internal filler rods (Figure 2). Both uncoated and barrier coated cladding with various heat treatments were used in this study (McKinnon 1992).

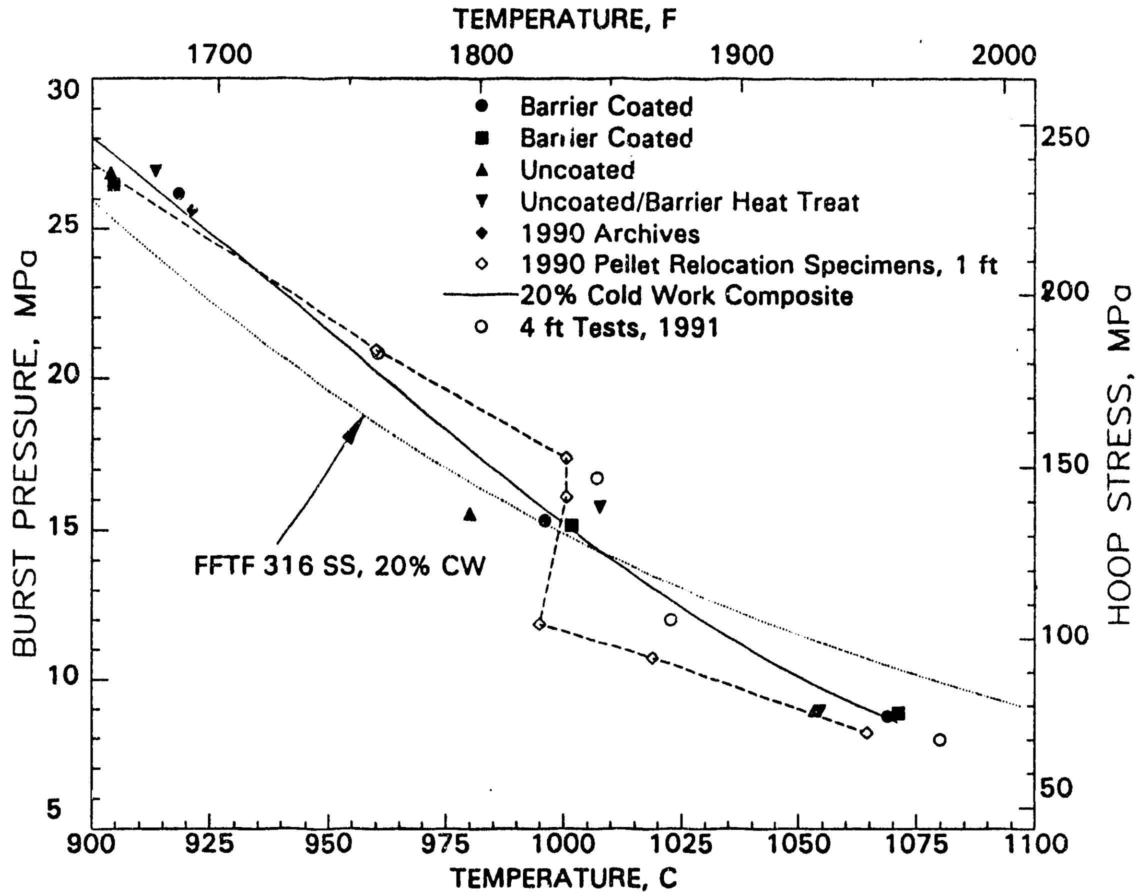

FIGURE 11. Comparison of 20% Cold Worked Cladding Strength to Prior Testing Results

Only one data point is shown for a 1990 archive specimen. The archive specimen was similar to the burst specimen but included an NPZ getter, $LiAlO_2$ pellets, and an inner liner in place of the filler rod (Figure 3). Figure 11 shows that the strength data obtained from the 4-ft specimens is consistent with that observed in previous tests.

4.2 BREACH CHARACTERISTICS

Dimensional changes are associated with cladding breach. The severity of damage to the rod and cladding was found to depend on the pressure in the rod at burst. The nature of the cladding breaches can be seen in Figures 12 through 15. At low internal pressure, the cladding is plastic and the breach

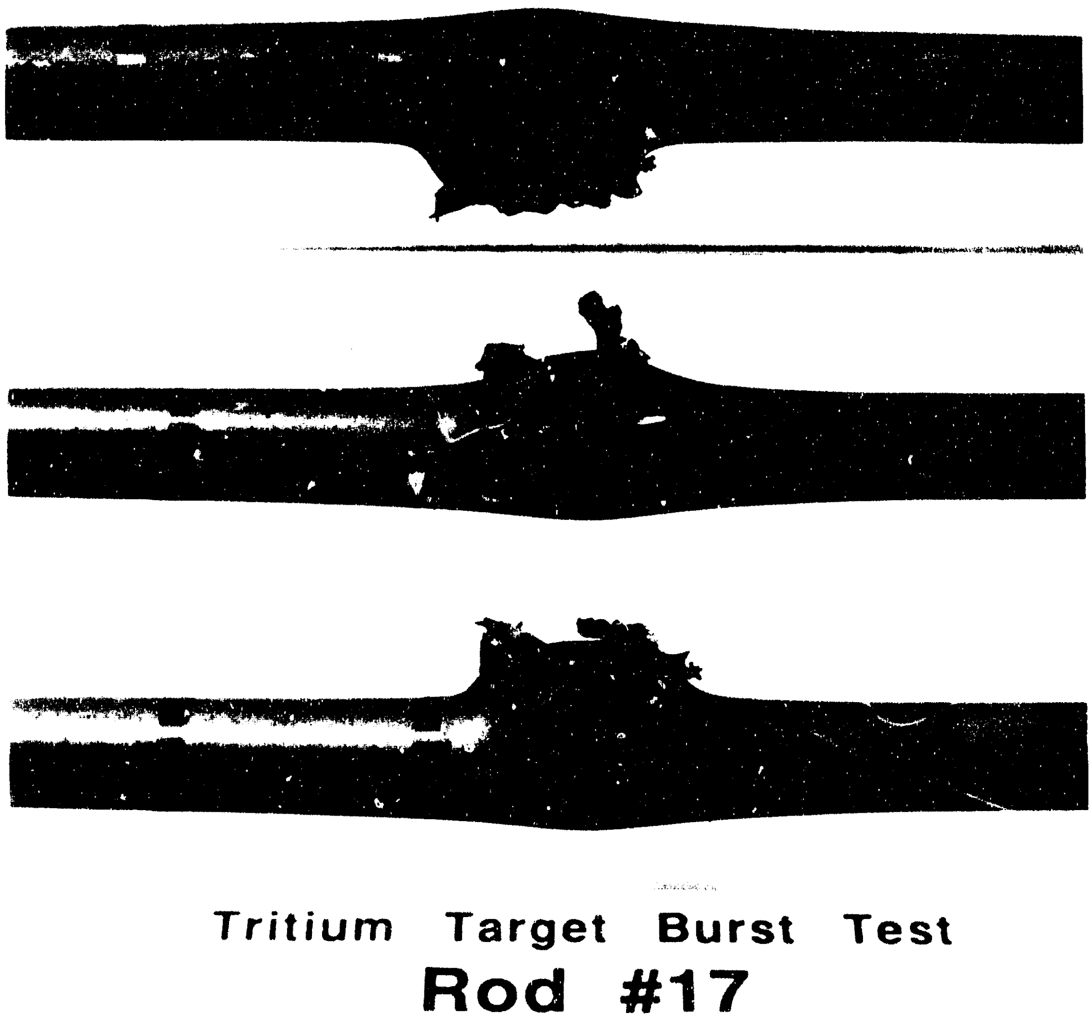

FIGURE 12. Burst Characteristics of Specimen 17 Burst at 8 MPa (1154 psi) and 1080°C (1976°F)

manifests itself as a bulge with a split. At high internal pressure, the cladding shears and is peeled back to release the pressure. The series of pictures of the breached cladding illustrates that the breach damage increases with pressure.

An effort was made to quantify the strain or diametrical change associated with each burst. This was done by comparing pretest and post-test diameter measurements near the burst location. The location of the pretest and post-test burst locations are shown in Figure 16. The location for the

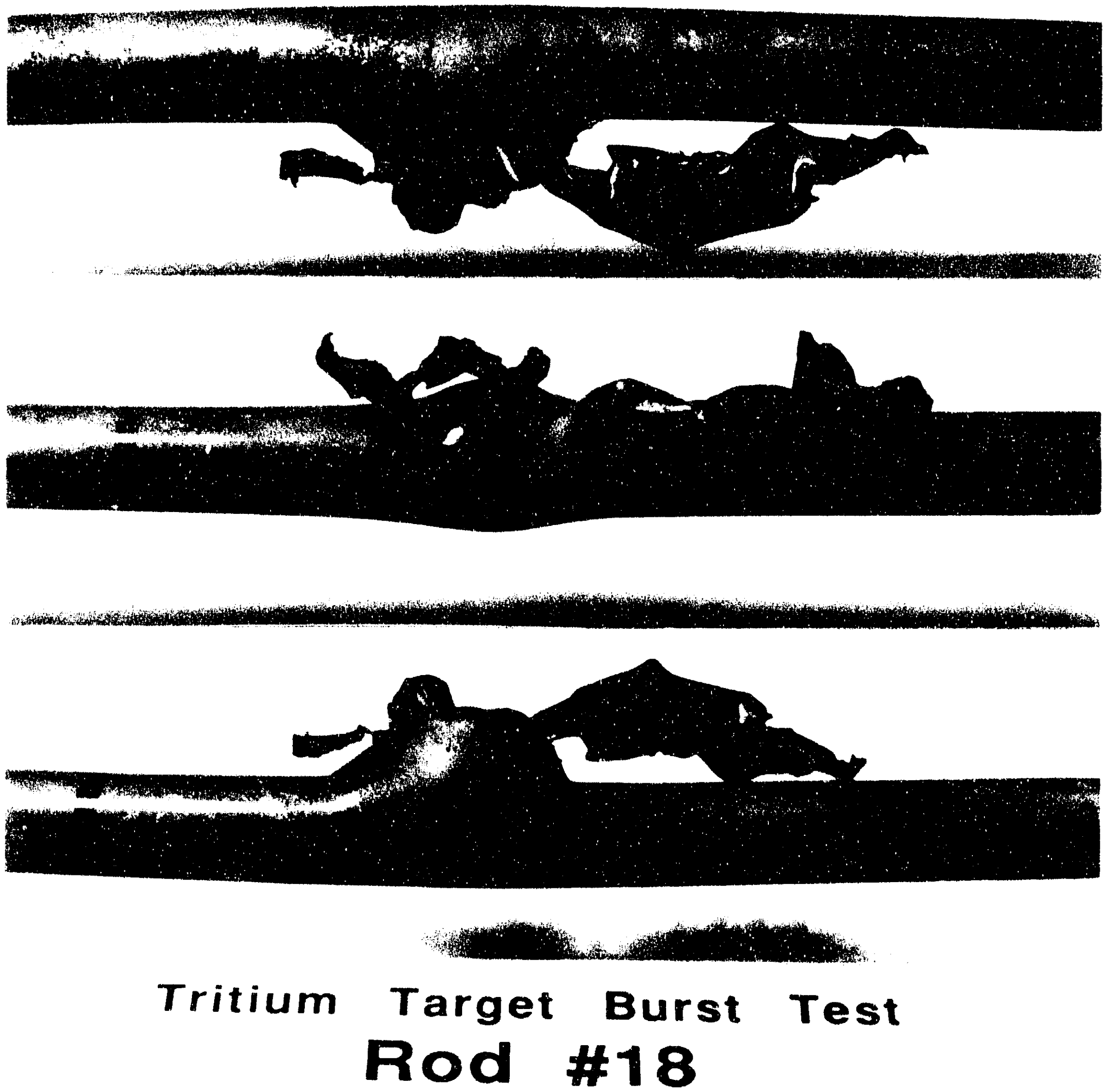

FIGURE 13. Burst Characteristics of Specimen 18 Burst at 12 MPa (1740 psi) and 1028°C (1873°F)

post-test measurement was selected to be as close to the end of a split or tear as possible (see Figure 16). Tabulated measurement values are presented in Appendix A. The post-test measurement location makes the data imprecise because it is difficult to obtain a consistent measurement location with respect to the center of the burst. At low pressures, specimens tend to bulge and may depressurize through a small split. At burst, the diametrical change at the end of the split is preserved. At high pressures, the tearing at the

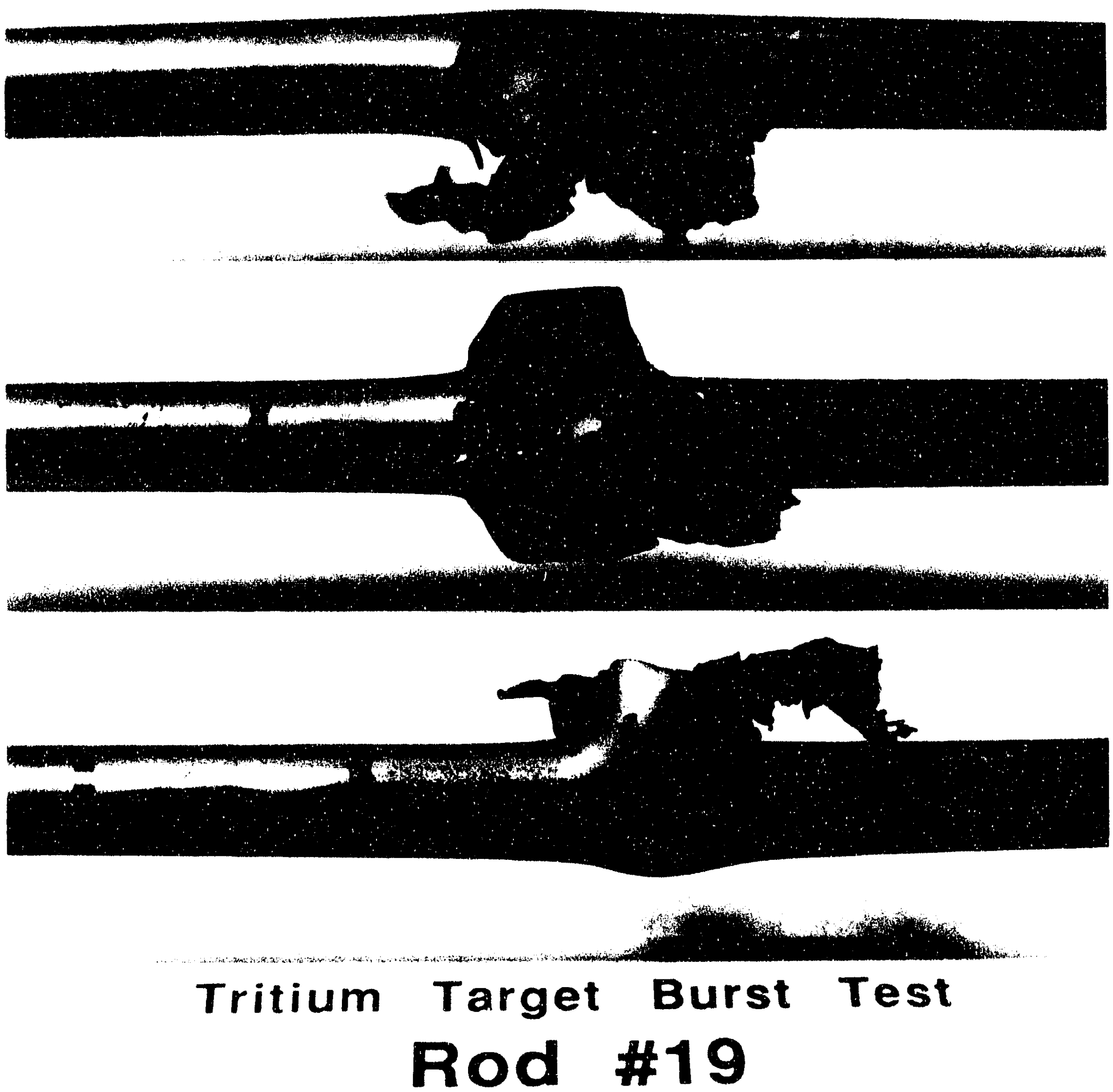

FIGURE 14. Burst Characteristics of Specimen 19 Burst at 16.7 MPa (2425 psi) and 1007°C (1845°F)

end of the split may mask the amount of strain that took place before the burst. The diametrical changes at the intact full tube location adjacent to the burst (Figure 16) are shown in Figure 17 (symbols '4').

Also shown on Figure 17 are the diametrical changes for other specimens tested as part of the TTDP. The four data points from the current study agree reasonably well with previous burst results. The 20% CW cladding has fairly

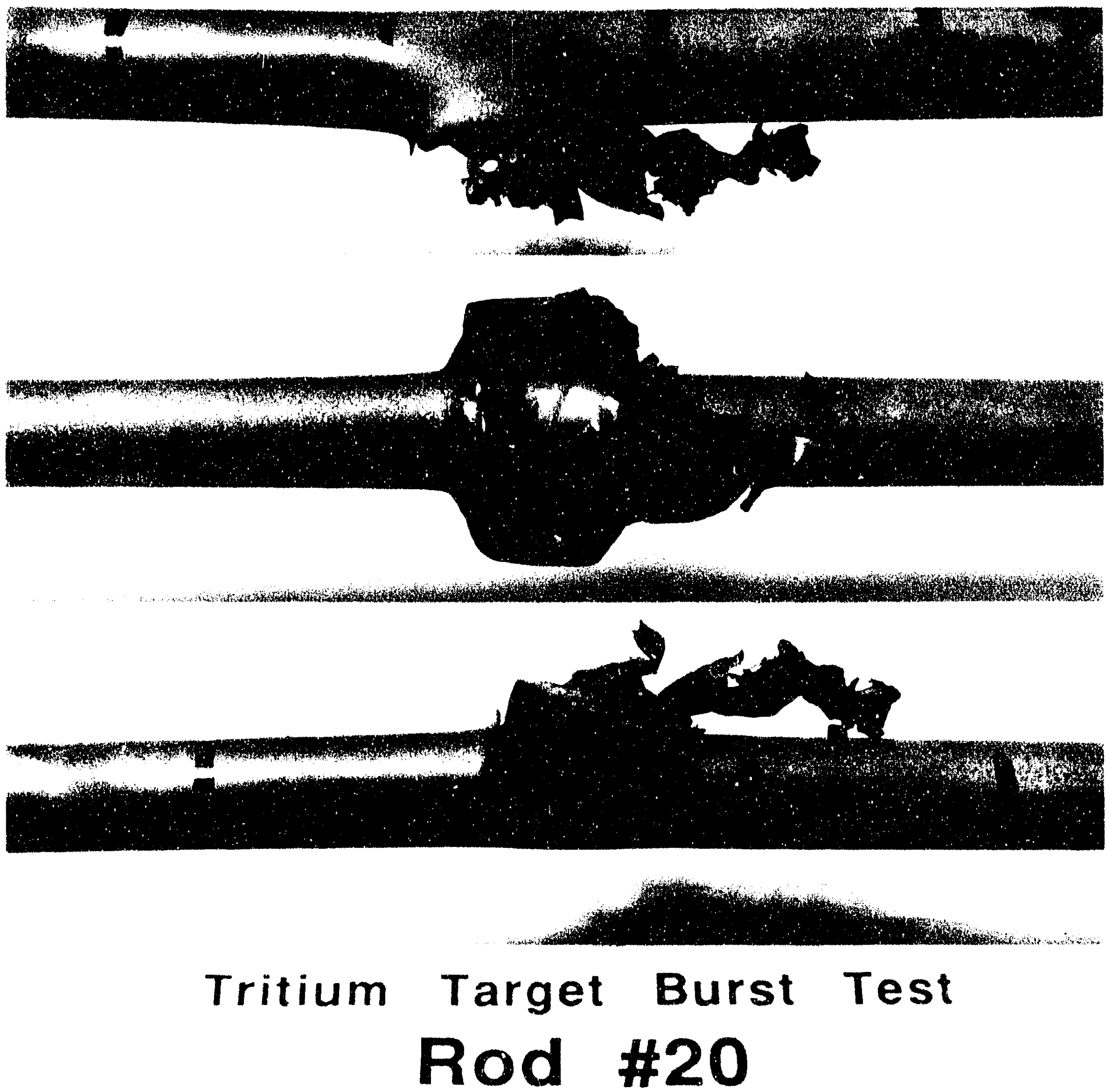

FIGURE 15. Burst Characteristics of Specimen 20 Burst at 20.8 MPa (3020 psi) and 960°C (1761°F)

constant burst strains up to about 950 to 1000°C. Above these temperatures, the cladding becomes more plastic and more strain is associated with the burst.

Specimen length measurements were made at the beginning of testing. Post-test length measurements were not made because length changes had not been observed in the previous study (McKinnon 1992) with shorter specimens.

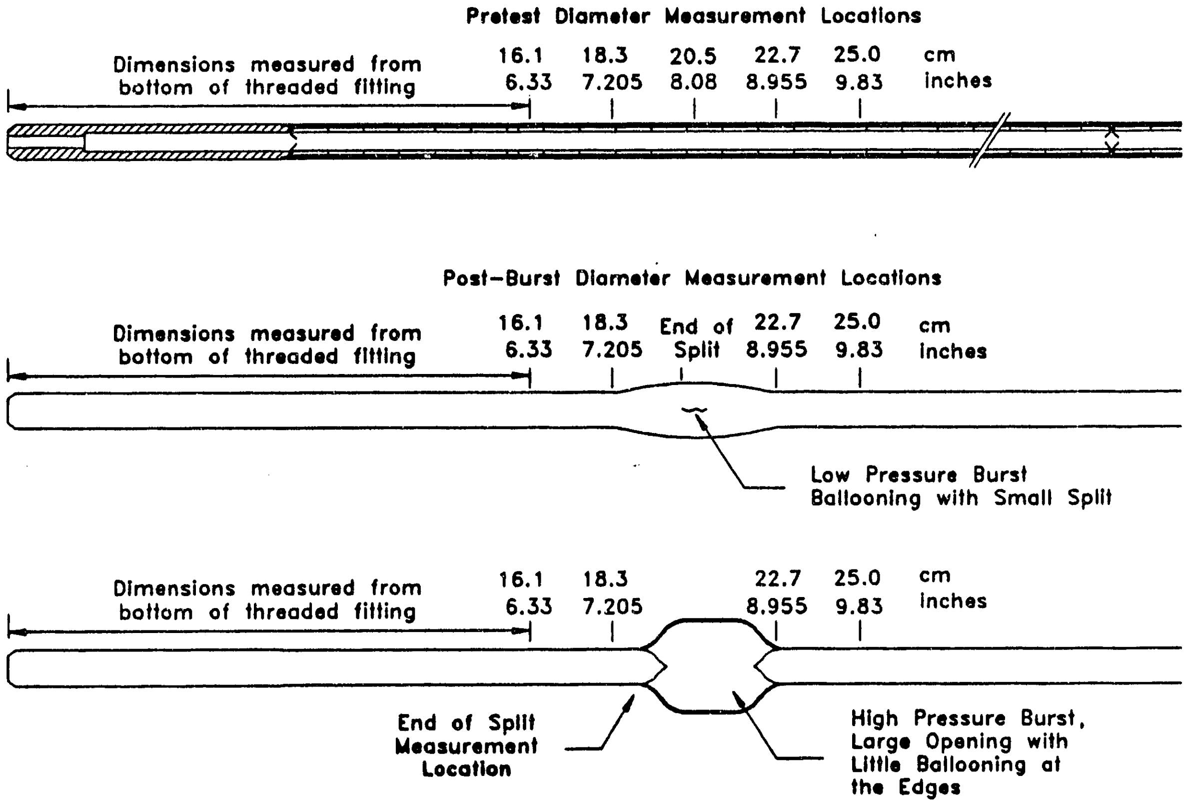

FIGURE 16. Pre- and Post-Test Diameter Measurement Locations

4.3 PELLET RELOCATION

Pellet relocation/dispersion was estimated based on weight changes of the specimen and interpretation of the radiographs, which allowed identification of missing components. During specimen assembly, the weights of the getter, inner liner, and $LiAlO_2$ pellets of the NPZ pencil were measured. The weights of each pencil and plenum spring assembly were also measured. After the specimens were assembled, a pretest weight was obtained and a pretest radiograph was taken for each specimen. After each specimen was burst tested, it was removed from the test stand and weighed, and a post-test radiograph was taken.

The post-test weights indicated that the pretest weights were in error. The difference between the pretest weights and the post-test weights exceeded

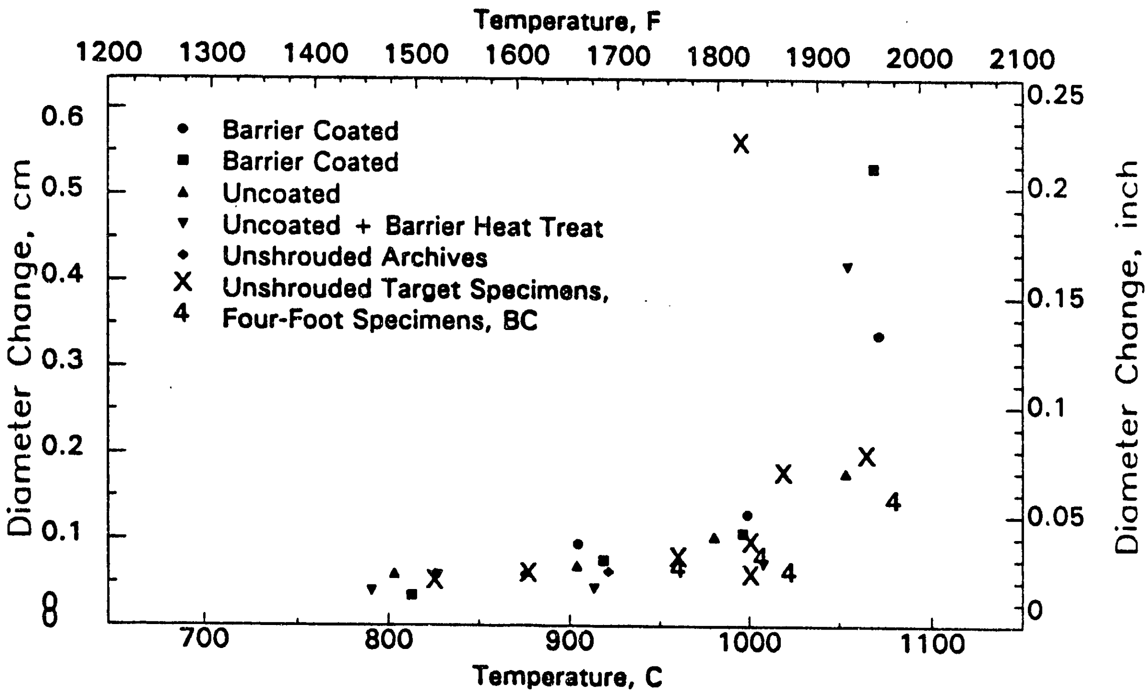

FIGURE 17. Target Rod Specimen Diameter Change During Burst Testing (20% CW Cladding)

the total weight of the four pencils and the plenum spring assembly. The pretest specimen weight was reconstructed by removing the remaining pencil material and plenum spring assembly from two of the specimens. The stainless steel cladding and end fittings were weighed, and then this weight was added to the pretest pencil and spring assembly weight of the specimen to calculate a pretest specimen weight. The average weight of the cladding and end fitting was added to the components of the other two specimens to estimate their pretest weights. Table 2 lists the reconstructed pretest and post-test weights of the specimens. Table 2 also lists the weight of pellet material expelled from the rod based on comparison of the post-test radiographs with the pretest radiographs. The weight of the rod after burst assumes that all the pellet material associated with increases in the plenum area or gaps between pencils was expelled from the rod during the bursts. The radiographs of the burst and plenum areas for each specimen are shown in Figures 18 to 21.

TABLE 2. Specimen Weight Before and After Burst Testing

Specimen Number	17	18	19	20
Reconstructed Pretest Weight, gm	332.87	332.83	332.78	332.27
Post-Test Weight Measurement, gm	331.78	328.50	328.70	328.50
Weight Lost during Burst, gm	1.09	4.33	4.08	3.77
Pretest Plenum Length, cm	15.9	15.9	15.95	15.95
Post-test Plenum Length, cm	18.1	21.5	21.40	21.95
Gaps between Pencils, cm	-	-	1.55	-
Increase in Plenum/Gap Length, cm	2.2	5.6	7.0	6.0
Pellet Weight Loss, gm (from Photos/Radiograph)	1.22	3.12	3.9	3.34
Burst Temperature, C	1080	1023	1007	960
Burst Pressure, MPa	8.0	12.0	16.7	20.8

Figure 22 compares the amount of material expelled from the specimens at burst. The locations of the lost material can be inferred from the post-test specimen radiographs shown in Figures 18 to 21. No loss of cladding was assumed; this is consistent with the weight loss information obtained from the previous study (McKinnon 1992).

Figure 22 shows an apparent peak in specimen weight loss between 12 and 16 MPa. The data are insufficient to establish the peak. Figure 22 does not show much difference between the pellet loss from the 1-ft and the 4-ft specimens. From an examination of the radiographs (Figures 18-21) it appears that the amount of material lost may have been controlled by the length of the heated zone. It appears that the pencils are driven toward the breach by the gas pressure. The getter material in the heated zone does not appear to have sufficient strength to withstand the axial driving force. As a result, the getter plasticly deforms and forms a bellows-type structure in the breach zone. As the brittle pellet material is exposed to the breach opening, it is broken up and expelled. Loss of the pellet material allows cooler portions of the pencil material to be driven to the breach area until a point is reached where the getter material is cool enough to have sufficient strength to withstand the axial driving force. At this point, the expulsion of pellet material stops. A post-test examination of pellets from two breached rods did not indicate pellet damage away from the breach opening. The pellets in the pencils adjacent to the breached pencil did not show any evidence of damage either, nor was pellet material below the breach driven to the breach.

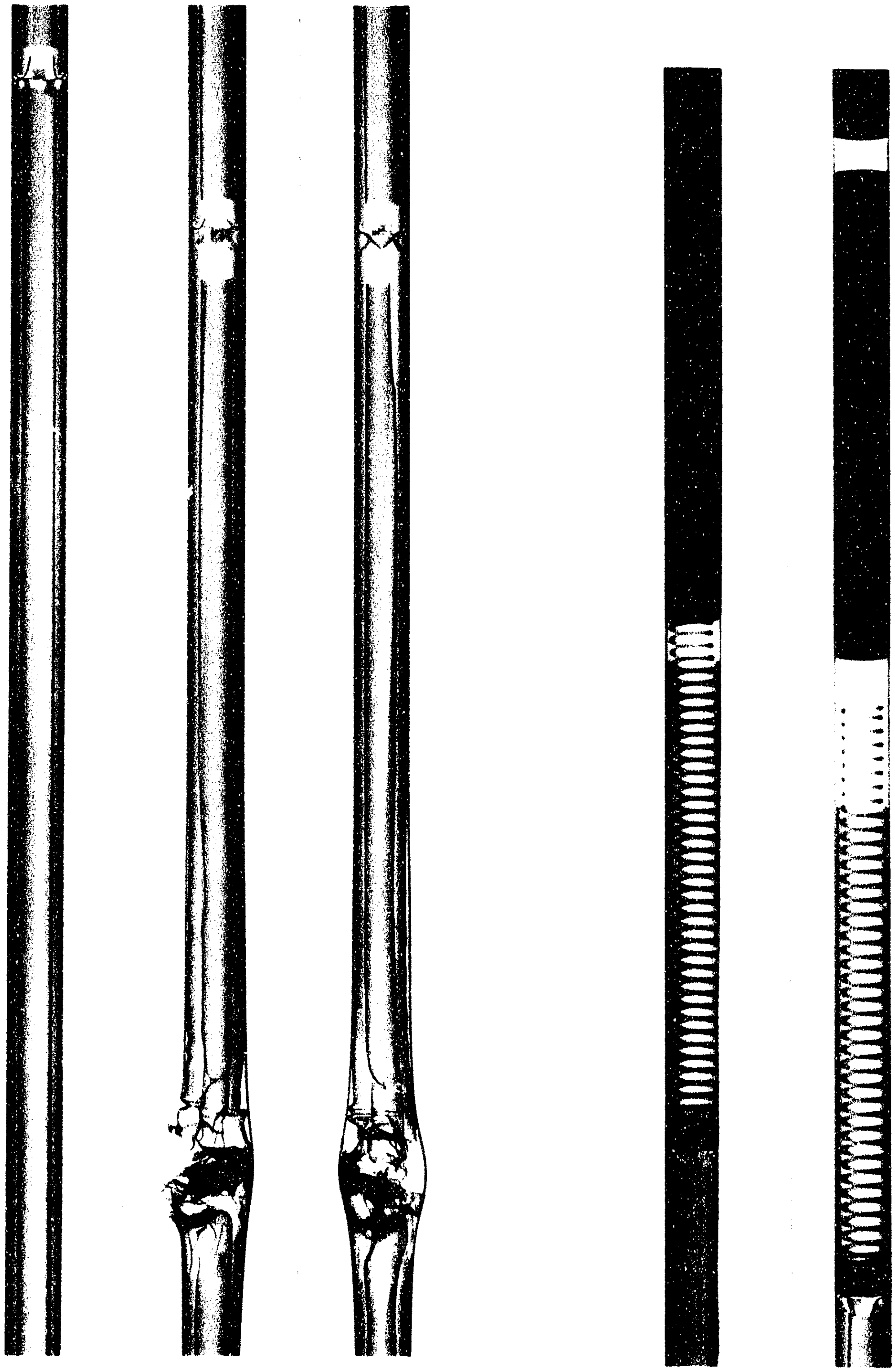

FIGURE 18. Radiographs of 4-ft Specimens After Burst Testing (burst pressure 8 MPa, temperature 1080°C)

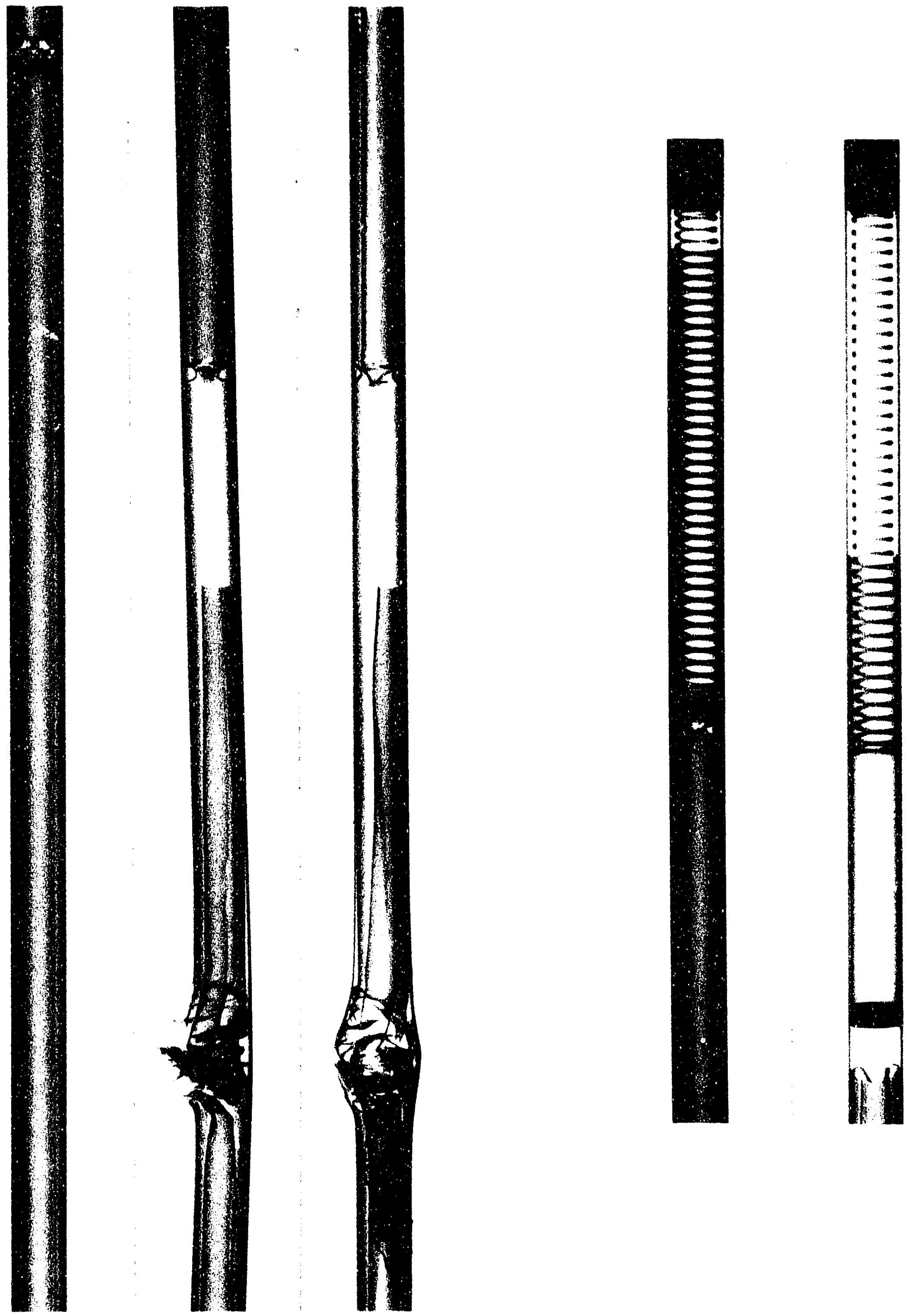

FIGURE 19. Radiographs of 4-ft Specimens After Burst Testing (burst pressure 12 MPa, temperature 1023°C)

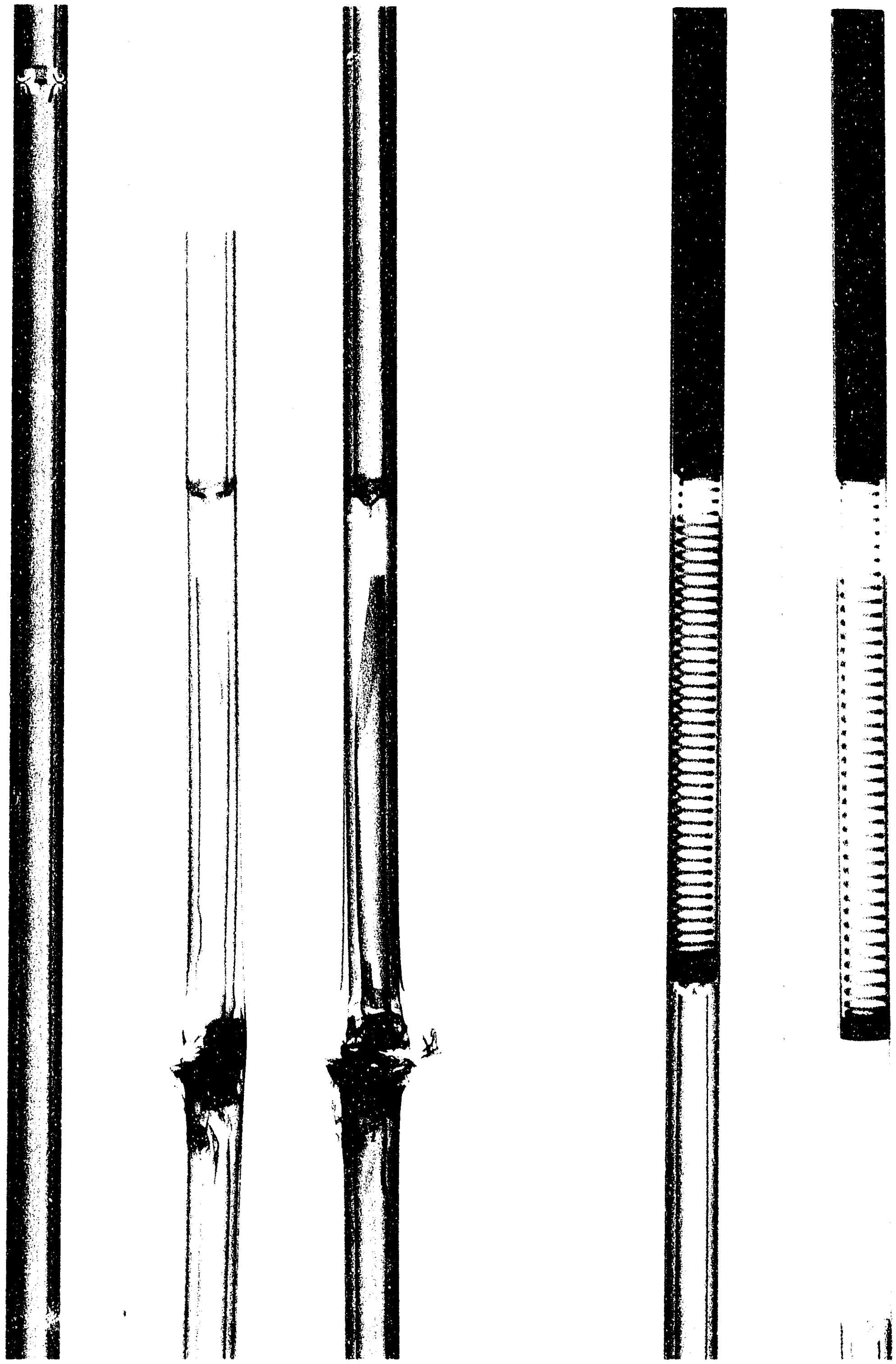

FIGURE 20. Radiographs of 4-ft Specimens After Burst Testing (burst pressure 16.7 MPa, temperature 1007°C)

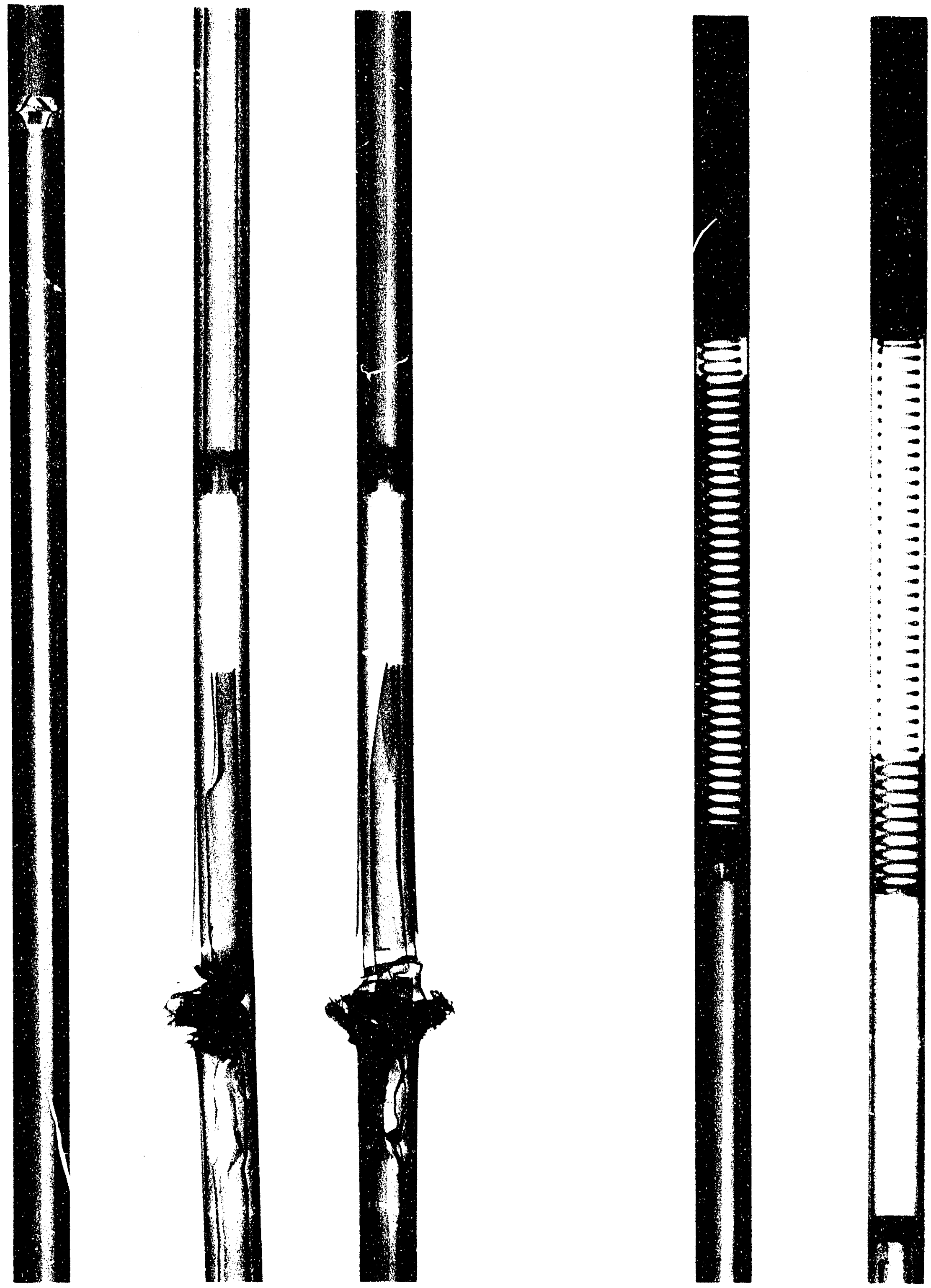

FIGURE 21. Radiographs of 4-ft Specimens After Burst Testing (burst pressure 20.8 MPa, temperature 960 °C)

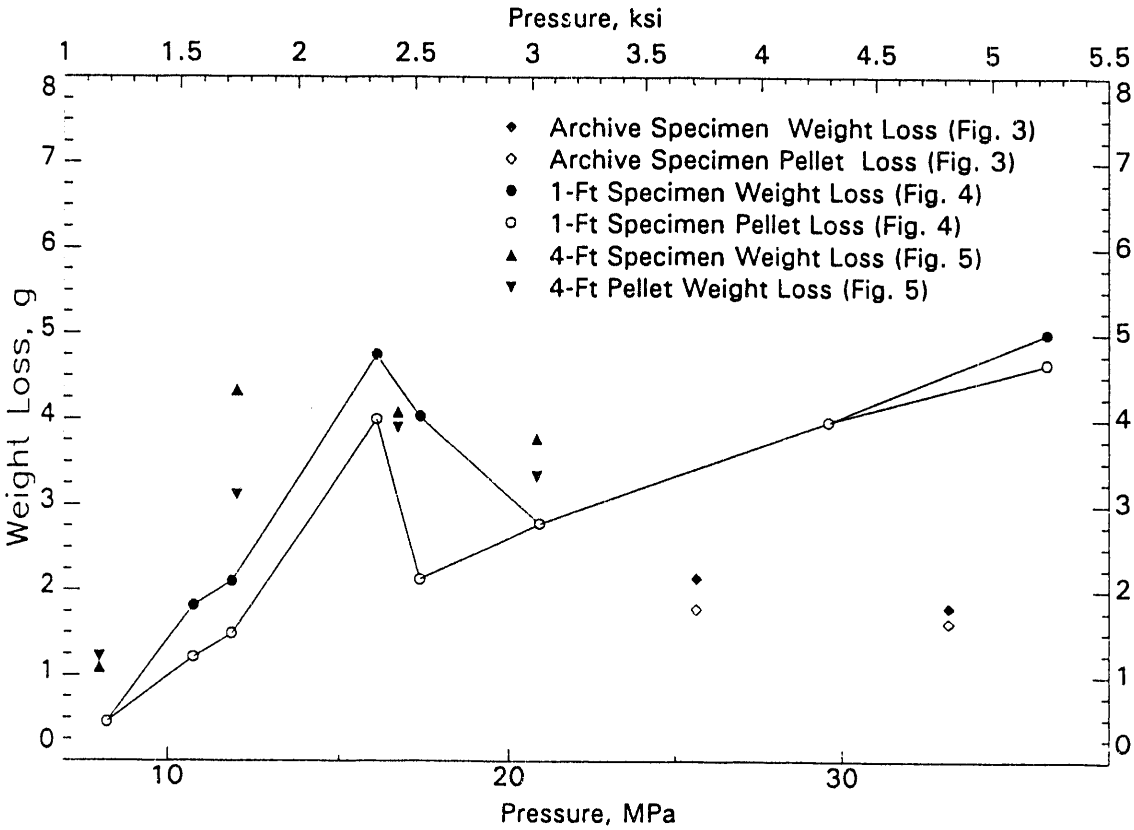

FIGURE 22. Comparison of Specimen Weight Loss During Burst Testing

5.0 REFERENCES

Carnes, J. R., and N. P. Kherani. 1987. Metal Hydrides. LA-10971-MS, Los Alamos National Laboratory, Los Alamos, New Mexico.

Heacock, H. W. 1991. Ramp Rate for LBLOCA NP LWR Target Breach Test. Letter report (H. W. Heacock to M. J. Clausen) dated May 29, 1991, Number 9153927. Westinghouse Hanford Company, Richland, Washington.

Hunter, C. W., R. L. Fish, and J. J. Homes. 1975. "Mechanical Properties of Unirradiated Fast Reactor Cladding during Simulated Overpower Transients," Nuc. Tech., Volume 27, p. 276-288, November 1975.

Marshman, S. C., S. G. McKinley, R. G. Clemmer, R. D. Bell, R. C. Britton, and W. J. Gray. 1991. Tritium Permeation Scoping Experiments. PNL-7843. Pacific Northwest Laboratory, Richland, Washington.

McKinnon, M. A. 1992. Cladding Strength and Pellet Relocation Testing Results from Tritium Target Rods. PNL-7912, Pacific Northwest Laboratory, Richland, Washington.

Omberg, R. P. 1991. Summary of the LOCA Temperature History. WHC-SD-WNP-PSAD-004, Rev. 0. Westinghouse Hanford Company, Richland, Washington.

Owczarek, J. A. 1964. Fundamentals of Gas Dynamics. International Textbook Company, Scranton, Pennsylvania.

Shiraga, S. S., and J. W. Weber. 1991. LWR Generic Target Rod Design Description. WHC-SD-WNP-DB-002, Rev. 0. Westinghouse Hanford Company, Richland, Washington

Weber, J. W. 1991. NP LWR Target Rod Design Description. WHC-SD-WNP-DB-002, Rev. 1. Westinghouse Hanford, Company, Richland, Washington.

APPENDIX A

TEST DATA

Specimen No. 17 Data Sheet

MATERIALS: ATR CRITICALS 1 Rod No. WK-31 (getters, pellets, and plenum spring source), SR-OD/PP-ID Coated Tube No. 1170, NPZ Getter Tube No.: 21

TEST SPECIMEN COMPONENTS

Lengths(inch):

Pencils: NPZ (Lower) 12.00, No NPZ (Bottom to Top) 12.01, 12.02, 12.01.

Specimen: Pretest 57.065

Weights (gm):

Getter from ATR Rod 6.5323, NPZ Getter 6.4650, Liner 2.8543, Pellets 16.991

Pencils: NPZ (Lower) 26.310, No NPZ (Bottom to Top) 26.407, 26.446, 26.291

Specimen: Pretest ~~619.9~~ Corrected 332.869, Post-test 331.78, Diff. 1.089

Specimen Internal Gas Volume: 39.6 ml

TC LOCATIONS

From threaded fitting end (inch) 6.58 , 7.33 , 8.08 , 8.83 , 9.58

DIAMETER MEASUREMENTS

Distance from End of Bottom Plug, inch	Circumferential Location, Degrees 0	45	90	135
Pretest Meas.				
6.33	0.3709	0.3708	0.3704	0.3707
7.205	0.3718	0.3706	0.3706	0.3705
8.08	0.3706	0.3709	0.3709	0.3706
8.955	0.3705	0.3703	0.3708	0.3704
9.83	0.3707	0.3704	0.3707	.03705
Post-test Meas.				
6.33	0.3745	0.3745	0.3745	0.3750
7.116	0.4280	0.4235	0.4275	0.4260
8.08	0.4145	0.4140	0.4190	0.4220
9.83	0.3955	0.3960	0.3960	0.3960

TEST DATA:

Test Date: Sep. 27, 1991, Time: 10:45 a.m., Heater Coil Number/ID: 1-4/24/90

Helium Charge Pres. 1030 psia., Burst Pres. 1154 psia., Burst Time 138.5 sec.

Soak Temperature 300°C, Ramp Rate 10°F/sec, Burst Temperature 1976°F,

Specimen No. 18 Data Sheet

MATERIALS: ATR CRITICALS 1 Rod No. WK-32 (getters, pellets, and plenum spring source), SR-OD/PP-ID Coated Tube No. 1166, NPZ Getter Tube No.: 35

TEST SPECIMEN COMPONENTS

Lengths(inch):

Pencils: NPZ (Lower) 11.97, No NPZ (Bottom to Top) 11.97, 11.97, 11.97.

Specimen: Pretest 57.065

Weights (gm):

Getter from ATR Rod 6.505, NPZ Getter 6.5283, Liner 2.8478, Pellets 16.941

Pencils: NPZ (Lower) 26.317, No NPZ (Bottom to Top) 26.340, 26.343, 26.444

Specimen: Pretest ~~619.8~~ Corrected 332.834, Post-test 328.5, Diff. 4.334

Specimen Internal Gas Volume: 39.7 ml

TC LOCATIONS: From threaded fitting end (inch) 6.58, 8.08, 9.58

DIAMETER MEASUREMENTS

Distance from End of Bottom Plug, inch	Circumferential Location, Degrees 0	45	90	135
Pretest Meas.				
6.33	0.3704	0.3703	0.3704	0.3703
7.205	0.3700	0.3700	0.3700	0.3700
8.08	0.3701	0.3700	0.3700	0.3702
8.955	0.3700	0.3701	0.3701	0.3701
9.83	0.3700	0.3701	0.3702	.03702
Post-test Meas.				
6.33	0.3745	0.3730	0.3750	0.3720
7.205	0.3740	0.3790	0.3945	0.3820
8.08	0.3845	0.3890	0.3990	0.3995
8.955	0.3740	0.3755	0.3770	0.3730
9.83	0.3695	0.3710	0.3710	0.3715

TEST DATA:

Test Date: Sep. 26, 1991, Time: 10:30 a.m., Heater Coil Number/ID: 1-4/24/90

Helium Charge Pres. 1560 psia., Burst Pres. 1740 psia., Burst Time 130 sec.

Soak Temperature 300°C, Ramp Rate 10°F/sec, Burst Temperature 1873°F,

Specimen No. 19 Data Sheet

MATERIALS: ATR CRITICALS 1 Rod No. WK-33 (getters, pellets, and plenum spring source), SR-OD/PP-ID Coated Tube No. 1168, NPZ Getter Tube No.: 41

TEST SPECIMEN COMPONENTS

Lengths(inch):

Pencils: NPZ (Lower) 11.97, No NPZ (Bottom to Top) 12.00, 12.00, 12.00.

Specimen: Pretest 57.065

Weights (gm):

Getter from ATR Rod 6.484, NPZ Getter 6.4630, Liner 2.8522, Pellets 16.975

Pencils: NPZ (Lower) 26.290, No NPZ (Bottom to Top) 26.330, 26.194, 26.551

Specimen: Pretest ~~620.0~~ Corrected 332.780, Post-test 328.7, Diff. 4.08

Specimen Internal Gas Volume: 39.6 ml

TC LOCATIONS: From threaded fitting end (inch) 6.58, 8.08, 9.58

DIAMETER MEASUREMENTS

Distance from End of Bottom Plug, inch	Circumferential Location, Degrees			
	0	45	90	135
Pretest Meas.				
6.33	0.3710	0.3710	0.3705	0.3705
7.205	0.3711	0.3708	0.3707	0.3702
8.08	0.3707	0.3705	0.3704	0.3705
8.955	0.3704	0.3705	0.3705	0.3706
9.83	0.3704	0.3704	0.3702	0.3705
Post-test Meas.				
6.33	0.3720	0.3740	0.3745	0.3765
7.205	0.3775	0.3820	0.3780	0.3780
7.55	0.3880	0.3745	0.3930	0.3900
8.382	0.3925	0.4020	0.4060	0.4010
8.955	0.3810	0.3800	0.3805	0.3810
9.83	0.3710	0.3715	0.3715	0.3710

TEST DATA

Test Date: Sep. 25, 1991, Time: 10:25 a.m., Heater Coil Number/ID: 1-4/24/90

Helium Charge Pres. 2160 psia., Burst Pres. 2425 psia., Burst Time 138.5 sec

Soak Temperature 300°C, Ramp Rate 10°F/sec, Burst Temperature 1845°F,

Specimen No. 20 Data Sheet

MATERIALS: ATR CRITICALS 1 Rod No. WK-34 (getters, pellets, and plenum spring source), SR-OD/PP-ID Coated Tube No. 1171, NPZ Getter Tube No.: 64

TEST SPECIMEN COMPONENTS

Lengths(inch):

Pencils: NPZ (Lower) 11.97, No NPZ (Bottom to Top) 12.00, 12.00, 12.00.

Specimen: Pretest 57.065

Weights (gm):

Getter from ATR Rod 6.607, NPZ Getter 6.4825, Liner 2.8427, Pellets 16.940

Pencils: NPZ (Lower) 26.265, No NPZ (Bottom to Top) 26.247, 26.188, 26.137

Specimen: Pretest ~~619.8~~ Corrected 332.277, Post-test 328.5, Diff. 3.777

Specimen Internal Gas Volume: 39.6 ml

TC LOCATIONS: From threaded fitting end (inch) 6.58, 8.08, 9.58

DIAMETER MEASUREMENTS

Distance from End of Bottom Plug, inch	Circumferential Location, Degrees			
	0	45	90	135
Pretest Meas.				
6.33	0.3701	0.3702	0.3703	0.3700
7.205	0.3700	0.3702	0.3702	0.3702
8.08	0.3700	0.3703	0.3702	0.3701
8.955	0.3700	0.3701	0.3703	0.3701
9.83	0.3700	0.3701	0.3702	0.3700
Post-test Meas.				
6.33	0.3710	0.3720	0.3730	0.3710
7.205	0.3755	0.3740	0.3810	0.3810
8.08	0.3855	0.3880	0.3920	0.3870
9.055	0.3965	0.3980	0.3950	0.3895
9.83	0.3715	0.3720	0.3720	0.3720

TEST DATA:

Test Date: Sep. 24, 1991, Time: 11:00 a.m., Heater Coil Number/ID: 1-4/24/90

Helium Charge Pres. 2700 psia., Burst Pres. 3020 psia., Burst Time 120.5 sec.

Soak Temperature 300°C, Ramp Rate 10°F/sec, Burst Temperature 1761°F,

APPENDIX B

ERROR ANALYSIS

APPENDIX B

ERROR ANALYSIS

Uncertainty limits in pressure and temperature were analyzed from data that was generated during transient burst testing. A computer program that calculates hoop stresses in thin wall target cladding was applied to the analysis of data uncertainty limits.

Data generated during the tritium target transient burst testing and tritium target transient safety testing was subject to the following uncertainty limits:

Thermocouple Uncertainty:	±9.375°C
Thermocouple Signal Conditioner Uncertainty:	±3.000°C
Total Uncertainty in Temperature Data:	±12.375°C
Heise Pressure Gauge Uncertainty:	±15.0 psig
Total Uncertainty in Pressure Data:	±15.0 psig

Thermocouple uncertainty was calculated from manufacturer's data as follows. The thermocouple is accurate to within ±2.2°C or ±0.75% of 1250°C, whichever is greater.

$$(1250°C) \times (0.0075) = 9.375°C$$

Since 9.375°C is greater than 2.2°C, the greater uncertainty of 9.375°C was applied to the calculation of total uncertainty for temperature measurement. (Note: Actual test temperature seldom exceeded 1060°C, which gives an actual uncertainty of 8°C).

To calculate the total uncertainty of the pressure data, the pressure transducer was first compared to the Heise gauge uncertainty of ±15.0 psig. According to the manufacturer's data, the pressure transducer accuracies are as follows:

±0.09% full scale, plus additional tolerances of the following:

±0.0056% full scale per degree F (from ambient) for thermal zero

±0.0017% full scale per degree F (from ambient) for thermal sensitivity.

For purposes of making calculations, assume that a 10,000 psi full-scale transducer is used, and that the temperature deviation of the transducer from ambient is negligible. Thus:

$$(10{,}000 \text{ psig}) \times (0.0009) = 9.000 \text{ psig}$$

$$(10{,}000 \text{ psig}) \times (0.000056/\text{psig-F}) \times (1.0^\circ\text{F}) = 0.560 \text{ psig}$$

$$(10{,}000 \text{ psig}) \times (0.000017/\text{psig-F}) \times (1.0^\circ\text{F}) = 0.170 \text{ psig}$$

Thus the total uncertainty in the pressure transducer is

$$(9.000 + 0.560 + 0.170) = 9.730 \text{ psig.}$$

Since the pressure transducer uncertainty is less than the Heise gauge uncertainty, the Heise gauge uncertainty of ±15.0 psig is used in the calculation of pressure data total uncertainty.

The uncertainty limits inherent in the transient testing data were considered acceptable for the following reasons:

1. The test data was more accurate than actual temperature measurements that would be available in the reactor core itself. That is, during a LOCA transient event, the temperature information that may be recorded or presented to the control room operator will have greater uncertainty than the temperature measurements made during transient testing.

2. The uncertainties in transient temperature measurement data are more accurate than, or at least as accurate as, the computer modeling results of postulated LOCA transients.

3. One can use existing data to predict the uncertainties in burst properties of the barrier cladding stainless steel alloy, and to show that this uncertainty is within the bounds of uncertainties in the temperature and pressure data from the barrier cladding transient testing.

4. Finally the data uncertainties are less than the applicable safety factors used for the design of core components and reactor systems.

B.1 SAMPLE CALCULATION OF BURST HOOP STRESS UNCERTAINTIES

The formula for hoop stress is:

$$\text{Hoop Stress} = \frac{P \times id}{2\ t}$$

where P = internal pressure, psig
id = tube inside diameter, inches
t = tube wall thickness, inches.

One can compare the nominal values of burst hoop stress and values at the limits of uncertainty to determine the relative effect of unknowns in pressure versus wall thickness. By examining the computation tables, it is apparent that wall thickness variations play a much greater role in hoop stress uncertainty than does pressure variation.

DISTRIBUTION

No. of
Copies

OFFSITE

12 DOE/Office of Scientific and
Technical Information

3 U.S. Department of Energy
Headquarters
Office of Light Water Reactor
Office of New Production
Reactor
1000 Independence Ave. SW
Washington, DC 20585
ATTN: S. G. Chalk
M. J. Clausen
W. F. Kelly

ONSITE

3 DOE Richland Field Office

E. A. Erichsen, A4-26
R. D. Filbert, A4-26
L. D. Romine, A4-26

4 Westinghouse Hanford Comapny

H. W. Heacock, HO-30
R. P. Omberg HO-40
R. J. Puigh, L6-39
E. S. Ruff, H5-67

No. of
Copies

35 Pacific Northwest Laboratory

R. P. Allen, P8-10
W. J. Apley, P8-34
D. L. Baldwin, P7-22
G. H. Beeman, P8-34 (5)
R. G. Clemmer, P7-14
J. L. Ethridge, P8-10
M. D. Freshley, P8-34
E. R. Gilbert, P8-34 (5)
N. E. Harding, P8-10
G. W. Hollenberg, P8-10
D. D. Lanning, P8-34
M. A. McKinnon, P8-10 (5)
J. P. Pilger, P8-34
H. G. Powers, P8-34
C. K. Thornhill, P7-43
G. L. Tingey, P8-34
S. E. Walker, P8-34
Publishing Coordination
Technical Report Files (5)

END

DATE FILMED

5/20/93